Title

THE ELECTRONIC STATE OF HEME IN CYTOCHROME OXIDASE II. REDOX POTENTIAL INTERACTIONS AND SPIN STATE BEHAVIOR OBSERVED IN REDUCTIVE TITRATIONS

Author

Babcock, Gerald T.

Publication Date

1977-10-01

Submitted to Journal of Biological Chemistry

LBL-6777
Preprint

THE ELECTRONIC STATE OF HEME IN CYTOCHROME OXIDASE II. REDOX POTENTIAL INTERACTIONS AND SPIN STATE BEHAVIOR OBSERVED IN REDUCTIVE TITRATIONS

Gerald T. Babcock, Larry E. Vickery, and Graham Palmer

October 1977

Prepared for the U. S. Department of Energy
under Contract W-7405-ENG-48

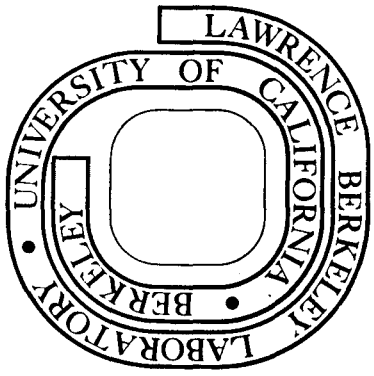

DISCLAIMER

THE ELECTRONIC STATE OF HEME IN CYTOCHROME OXIDASE II. REDOX POTENTIAL INTERACTIONS AND SPIN STATE BEHAVIOR OBSERVED IN REDUCTIVE TITRATIONS

Gerald T. Babcock, Larry E. Vickery[*, ϕ] and Graham Palmer[†]

Department of Chemistry, Michigan State University
East Lansing, MI 48824, [*]Laboratory of
Chemical Biodynamics, University of California
Berkeley, CA 94720 and [†]Department of
Biochemistry, Rice University, Houston, TX 77005

[ϕ]Present Address: Department of Physiology, College of Medicine, University of California, Irvine, CA 92717.

ABSTRACT

Magnetic circular dichroism (MCD), electron paramagnetic resonance (EPR) and optical absorption spectroscopies have been used to monitor the concentrations of oxidized and reduced heme and copper during stoichiometric reductive titrations of purified beef heart cytochrome oxidase. The MCD data are deconvoluted to obtain the concentrations of reduced cytochromes $\underline{a}$ and $\underline{a}_3$ during the titrations; analysis of the EPR spectra provides complementary data on the concentrations of the EPR detectable species.

For the native enzyme in the absence of exogenous ligands, cytochromes $\underline{a}$ and $\underline{a}_3$ are reduced to approximately the same extent at all points in the titration. The reduction of the EPR detectable copper, on the other hand, initially lags the reduction of the two cytochromes but in the final stages of the titration is completely reduced prior to either cytochrome $\underline{a}$ or $\underline{a}_3$. These non-Nernstian titration results are interpreted to indicate that the primary mode of heme-heme interaction in cytochrome oxidase involves shifts in redox potential for each of the two cytochromes such that a change in oxidation state for one of the hemes lowers the redox potential of the second heme by approximately 135 mV. In these titrations high-spin species are detected which account for 0.25 spins/oxidase maximally. Evidence is presented to indicate that at least some of these signals can be attributed to cytochrome $\underline{a}^{3+}$ which has undergone a low-spin to high-spin state transition in the course of the

titration.

In the presence of carbon monoxide the redox properties of cytochromes $\underline{a}$ and $\underline{a}_3$ are markedly altered. The $\underline{a}_3^{2+} \cdot CO$ complex is fully formed prior to reduction of either cytochrome $\underline{a}^{3+}$ or the EPR detectable copper. The $g = 3$ EPR signal attributed to cytochrome $\underline{a}^{3+}$ decreases as the MCD intensity of cytochrome $\underline{a}^{2+}$ increases; no significant high-spin intensity is observed at any intermediate stage of reduction. We interpret these Nernstian titration results to indicate that in the presence of ligands the redox potential of cytochrome $\underline{a}$ relative to cytochrome $\underline{a}_3$ is determined by the redox state of cytochrome $\underline{a}_3$ stabilized by the ligand: if ligand binding occurs to reduced cytochrome $\underline{a}_3$ then cytochrome $\underline{a}$ titrates with a low potential; cytochrome $\underline{a}$ titrates with a high potential if oxidized cytochrome $\underline{a}_3$ is stabilized by ligand binding.

INTRODUCTION

Despite the intensive efforts of the past 40 years (1) considerable uncertainty exists as to the basic mechanism by which cytochrome oxidase catalyzes the four electron reduction of dioxygen to two molecules of water. It has been established that each of the four metal components of the protein, 2 heme *a* bound iron atoms and 2 copper atoms, exists in a unique environment. Further, the 2 heme *a* components have been distinguished on the basis of their respective ligand binding properties: cytochrome a_3 binds ligands in both the oxidized (e.g., CN^-, N_3^-) and reduced (e.g., CN^-, CO, NO) states whereas cytochrome *a* does not bind ligand in either redox state. These observations, based primarily on absorption spectroscopy as the experimental technique, led to postulation of the model for cytochrome oxidase, summarized by Lemberg (1), which is referred to as the dualistic or classical model. Its basic tenets include (a) cytochrome *a* is low-spin in its oxidized and reduced forms and in the reduced protein, exhibits a Soret maximum with an intensity some five-fold the intensity of the α-band. (b) The Soret:α ratio of reduced cytochrome a_3 is much larger (ca. 10:1) due to its weak α band absorbance, but the ascription of this heme component as high-spin is equivocal. No provision is included in the model for interaction of any kind between the four metal components of the oxidase.

We (2) have recently interpreted our MCD (3) and published magnetic susceptibility (4,5) data to indicate that cytochrome *a* is low-spin and cytochrome a_3 is high-spin in both the fully

oxidized and fully reduced states of the enzyme as anticipated by the classical model. However, extensive evidence has accumulated suggesting that at least two types of metal-metal interaction are operative in the protein. The first of these interactions was originally postulated by Van Gelder and Beinert (6) on the basis of EPR observations; it involves an antiferromagnetic coupling between high-spin cytochrome a_3^{3+} and one of the oxidized copper atoms (designated Cu_u^{2+}) such that the effective magnetic moment in the fully oxidized enzyme is decreased from the value anticipated for the sum {S = 5/2 + S = 1/2} for a noninteracting system, to S = 2 for the coupled system.

Our MCD results provided strong support for this magnetic coupling hypothesis and led us to propose a model for the enzyme which is able to rationalize a number of observations in the literature, including earlier EPR, (6) Mossbauer (7) and magnetic susceptibility data (4,5). In the model we propose that cytochrome a_3^{3+} and Cu_u^{2+} share a bidentate ligand, a bridging imidazole group from histidine, and that the expected EPR signals from cytochrome a_3^{3+} and Cu_u^{2+} are quenched by the resulting antiferromagnetic coupling. As a consequence EPR signals are observed only from cytochrome a^{3+} and the EPR detectable copper, Cu_d^{2+}, in the oxidized enzyme. Some of the fundamental predictions of our model have recently been substantiated by room temperature magnetic susceptibility measurements by Falk et al. (8) who find values for the susceptibility of the oxidized

and reduced enzyme as predicted (2).* These results also confirm our estimate, from MCD data (3), of the strength of the antiferromagnetic interaction ($J > 200\ cm^{-1}$).

The second type of metal-metal interaction in cytochrome oxidase was observed initially by Minneart (9) who noted anomalies in the reductive titration behavior of the enzyme. Wilson and coworkers (10,11), using potentiometric titration of the enzyme as the primary technique, have extensively explored this behavior. To fit their titration data to well-defined, Nernstian behavior, they postulated extensive interaction between the two hemes *a* of the protein such that the redox and ligation state of one of the hemes significantly altered the spectral behavior and, to a lesser extent, the redox potential of the second heme. For example, in the fully reduced enzyme cytochromes *a* and a_3 were postulated to have approximately equal extinction coefficients at 605 nm. Binding of carbon monoxide by cytochrome a_3 was postulated to increase the extinction coefficient of cytochrome *a* by a large factor. Malmstrom (12) and Nicholls and coworkers (13,14) pointed out an alternative explanation for these data; this requires that the spectral properties of the two hemes are essentially independent of one another and heme-heme interaction

---

*We have just completed magnetic susceptibility measurements on cytochrome oxidase and several of its derivatives over the temperature range 7°-250°K. The results of these measurements are in excellent agreement with the requirements of our model. (M. Tweedle, G. T. Babcock, L. Garcia-Iniguez, L. Wilson and G. Palmer, to be submitted).

is manifested primarily by interdependent redox properties for the two iron atoms. This second possibility, heme-heme interaction via changes in redox properties, has been elaborated recently by Wikström et al. (15) as the neoclassical model.

The resolution of the mechanism by which this heme-heme interaction takes place has been hampered by a lack of experimental techniques with the sensitivity and ease of application necessary to probe the system effectively. Optical spectroscopy is ambiguous because of the nature of the two conflicting models; EPR provides concentration data on oxidized species only and the magnetic coupling between cytochrome a_3^{3+} and Cu_u^{2+} further limits the information available by this approach; magnetic susceptibility measurements usually require very high concentrations of enzyme and fairly restrictive sample handling techniques (see, however, Reference 8) and the information obtained characterizes the system as a whole, which does provide a test for specific models for the enzyme, but does not give specific information on individual components. To overcome this difficulty, we have recently introduced the use of magnetic circular dichroism in the study of cytochrome oxidase (2,3). The principal advantage of this spectroscopy is that it provides spin-state information on both oxidized and reduced cytochrome oxidase and, furthermore, can easily be quantified. In previous publications, we have characterized the MCD properties of reduced and oxidized cytochrome oxidase and a number of its inhibitor complexes. One of the conclusions reached in this work was that the MCD spectra of these compounds showed little evidence for a heme-heme

interaction scheme in which the spectral parameters of the two cytochromes were strongly interdependent.

In the experiments described here, we have used MCD in conjunction with EPR spectroscopy to monitor changes in the concentrations of cytochromes *a* and a_3 and the EPR detectable copper during stoichiometric reductive titrations of the enzyme. Our results demonstrate that the primary mode of heme-heme interaction involves shifts in redox potential for each of the two cytochromes such that a change in oxidation state for one of the hemes lowers the redox potential of the second heme; the result is non-Nernstian titration behavior. In the presence of heme binding ligands (e.g., CO or N_3^-) each of the cytochrome titrates independently. In these cases the redox potential of cytochrome *a* relative to cytochrome a_3 is determined by the redox state of cytochrome a_3 stabilized by the added ligand: if cytochrome a_3^{2+} is favored by ligand binding, cytochrome a^{3+} titrates with a low potential; the converse situation obtains if cytochrome a_3^{3+} is stabilized. Finally we show that the *g*6 EPR signals, observed at intermediate levels of enzyme reduction, do not arise solely from cytochrome a_3^{3+} (2,6).

MATERIALS AND METHODS

Solubilized beef heart cytochrome oxidase was obtained as described by Hartzell and Beinert (16). The spectroscopic ratios for solubilized product were in agreement with those cited by Lemberg (1). In addition, as noted by Gibson et al.

(17), we have found the ratio $\frac{A_{red}(443)}{A_{red}(420)}$ to be an especially sensitive indicator of the integrity of these preparations; for protein used in the experiments described here, this ratio was 2.40 or greater. Enzyme concentration on a per heme *a* basis was determined using ε_{red} (443 nm) = 106 mM^{-1} cm^{-1}. The temperature was maintained at 11°C unless noted.

Optical spectra were obtained with either Cary 14 or Cary 17 spectrophotometers. MCD spectra were recorded by using the computer interfaced spectrophotometer described by Sutherland et al. (18). The calibration of the instrument and experimental operating conditions have been described previously (3). The maximum absorbance of cytochrome oxidase solutions used in obtaining Soret MCD spectra did not exceed 1.2. EPR spectra were recorded at X-band using a Varian E-6 spectrometer operated at approximately 12°K. Instrumental conditions in recording EPR spectra were as follows: (a) g=2 signal: 0.5 mW power, 10G modulation amplitude, (b) g=3 and g=6 signals: 3 mW power, 20G modulation amplitude.

Reductive titrations were carried out in all glass titration vessels. Stock solutions of sodium dithionite, standardized by titration of lumiflavin-3-acetate, were used as the reductant. The titrating vessel used in experiments in which both optical and MCD changes were recorded as a function of reduction is similar to that described by Burleigh et al. (19). Their design has been modified so that the gas lock and rubber septum on the titrating port is replaced by a female glass stopper. After anaerobiosis has been achieved, this stopper is removed

under a stream of argon and the dithionite containing syringe is inserted. The titrating vessel used in experiments in which both optical and EPR changes were recorded as a function of reduction has recently been described in detail by Palmer (20). The experimental protocol in both sets of experiments is identical. The protein is loaded into the titrating vessel and made anaerobic by gentle agitation under an argon atmosphere followed by evacuation and replacement of the argon. This operation is repeated six times to insure complete anaerobiosis. The optical spectrum of the oxidized enzyme is then recorded and, subsequently, the MCD spectrum is taken or an aliquot is removed and frozen for later EPR analysis. A known amount of dithionite solution is added, the optical spectrum is monitored until reductant induced changes are complete and, subsequently, the MCD spectrum or EPR sample is taken. The optical spectrum recorded for each MCD or EPR sample monitors the stability of the sample during the titration and is the touchstone which allows us to compare results from the two different techniques.

Quantitation of the MCD results is described in the Results section. Quantitation of the g=6 EPR signal intensity was carried out using the truncated second integral described by Aasa et al. (21) with metmyoglobin fluoride as the standard. Metmyoglobin fluoride concentration was determined optically using extinction coefficients, ε=9.2 mM^{-1} cm^{-1} at 604 nm and ε=9.9 mM^{-1} cm^{-1} at 487 nm (22). The EPR spectra of the standard and of one sample taken during a reductive titration are shown in Figure 1; application of the quantitation procedure above followed by correction

for the concentration difference between the standard and the oxidase sample results in a high spin concentration of 0.2/oxidase for this particular partially reduced sample. The intensity of the g=3 signal in the fully oxidized enzyme was taken as indicating 1.0 spins/oxidase molecule (21); the amplitude of the g=3 signal for subsequent samples was determined by comparison with the fully oxidized spectrum. Quantitation based on the first integral of the g=3 peak agreed within 3% with quantitation based on the g=3 peak height. The amplitude of the g=2 signal in the fully oxidized enzyme was taken as indicating 0.8 spins/oxidase (16,21). Signal intensities for partially reduced samples were determined by comparison of the trough intensity in the g=2 region with that exhibited by the fully oxidized sample.

RESULTS

Reductive Titration Under an Inert (Argon) Atmosphere

Figure 2 shows absorbance changes in the 500-630 nm region observed during a combined optical/EPR reductive titration of cytochrome oxidase under an argon atmosphere. An isosbestic point is observed at 621 nm; the increase in absorbance at 605 nm is approximately linear with the degree of reduction. These data, along with normalized absorbance changes observed at 830 nm and 443 nm, are summarized in the inset. The progress of the changes at 605 nm and 443 nm, corresponding to the reduction of heme a iron, are similar whereas the absorbance at 830 nm does not begin to decrease until approximately 1.0 electrons/

oxidase have been added. Data similar to these have been reported previously (23-25); the lag in onset for the changes at 830 nm has been interpreted to indicate that the redox potential for the copper responsible for most of the absorbance changes at this wavelength is more negative than that of (at least) one of the cytochrome components of the oxidase.

EPR data obtained during the same titration showed that in the oxidized enzyme a strong g=3 signal is observed along with a small g=4.3 signal which arises from adventitiously bound, non-physiological ferric iron (16,21). There is also a small g=6 signal, which when quantified, represents less than .02 spins/oxidase. Partial reduction results in a decrease in the g=3 signal intensity and an increase in the g=6 signal intensity (6). Inspection of the resonance in the g=6 region (see Figure 1) shows that these signals arise from high-spin ferric iron in two different environments, the more rhombic component having lesser amplitude but comparable total intensity to the axial species. Wilson and coworkers, noting that the two g=6 species responded in the same way to changes in redox potential, pH and added ligands, attributed the signals to a room temperature equilibrium between two high-spin forms of ferric iron which is maintained as the sample is cooled to EPR operating temperatures (26,27). During reoxidation experiments using ferricyanide or porphyrexide as oxidants, Beinert et al. (28,29) have also observed axial and rhombic high-spin EPR signals. The intensity of the signals observed by Beinert et al., however, is much greater (accounting for as much as 50% of the total heme a of the sample)

than is usually observed during reductive titrations and, moreover, under their conditions the two high-spin components are not in rapid equilibrium.

The quantitation of the EPR resonances observed during the course of the titration is shown in Figure 3. The low-spin iron (g=3) signal decreases monotonically throughout the titration; the g=2 signal exhibits an initial lag and then decreases monotonically. Comparison of the changes in the g=2 signal intensity (Figure 3) with the normalized decrease in the absorbance at 830 nm (Figure 2) shows a close correspondence between the two and supports the assignment of these parameters to the same species, viz. Cu_d^{2+} (10,25). As observed by Van Gelder and Beinert (6) and subsequently confirmed in both reductive (21,30) and potentiometric titrations (26,31), the g=6 signal is maximal at approximately half reduction of the enzyme, although at this point the high-spin concentration is only 24% of the total enzyme concentration. As noted above, the intensity of the high-spin signals observed during oxidation and reduction of cytochrome oxidase is strongly dependent on the experimental protocol. The cause of this variation is, at present, unclear. However, the principal goal of the research described here is to correlate titration results in EPR experiments (which provide concentration data on oxidized species) with titration results in MCD experiments (which we use here to provide concentration data on reduced species) to gain more complete information on the thermodynamics of cytochromes a, a_3 and the copper atoms.

The quantitation of high-spin heme species shown in Figure 3 is typical of our results in a number of different titrations, i.e., maximal high-spin concentrations in the range 20-30% of the total enzyme concentration at neutral pH. The consistency with which we observe these data provides confidence in the validity of the MCD/EPR correlations presented below.

We have recently demonstrated that the MCD spectrum of reduced cytochrome oxidase can be interpreted as the sum of two MCD curves: an intense asymmetric MCD band very similar to that exhibited by deoxymyoglobin which we assigned to high-spin cytochrome a_3^{2+} and a weaker, more symmetric MCD band which was assigned to diamagnetic low-spin cytochrome a^{2+} (2,3). Moreover, inhibitor studies showed that the MCD spectrum of cytochrome a^{2+} is independent of both the spin and redox state of cytochrome a_3. In the resting enzyme only low-spin cytochrome a^{3+} has significant MCD intensity; cytochrome a_3^{3+} was assigned to the high-spin state on this basis (32). We have used the spectra from our earlier work together with the conclusion that the MCD parameters for cytochromes a and a_3 show little evidence for spectral heme-heme interaction to compute the individual spectra for the hemes of cytochrome oxidase (Figure 4). Low-spin cytochrome a^{3+} shows a derivative shape C term centered around 427 nm; the MCD spectrum of cytochrome a^{2+} is temperature independent (3,33) and shows a maximum at 452 nm. In the absence of ligands cytochrome a_3^{3+} is high-spin and, as expected, shows very weak MCD intensity; addition of CN^- generates the low-spin cytochrome $a_3^{3+} \cdot CN^-$ complex which has a derivative-shape MCD

spectrum centered around 427 nm. High-spin cytochrome a_3^{2+} has an intense, temperature dependent MCD spectrum with a maximum at 447 nm, conversely the low-spin cytochrome $a_3^{2+} \cdot CO$ has very weak MCD intensity. From these individual spectra the MCD parameters for cytochromes a^{2+} and a_3^{2+} have been obtained (Table I) and are used below to deconvolute the Soret MCD spectra of cytochrome oxidase samples prepared at intermediate levels of reduction.

Figure 5 shows absorption (bottom) and MCD (top) spectra in the Soret region obtained during the course of a reductive titration carried out under argon. The MCD data show that the peak at ca. 450 nm increases with the first reducing equivalents entering the molecule and that during the course of the titration this MCD maximum undergoes a slight blue shift, from 450.5 nm for the first addition to 447 nm for the fully reduced enzyme. Deconvolution of this set of spectra allows the concentrations of cytochromes a_3^{2+} and a^{2+} to be plotted as a function of the number of electrons added (Figure 6). The observation that both hemes are reduced to the same extent at all stages of the titration shows that the two hemes of the oxidase exhibit very similar redox properties. (The lack of an isosbestic point in the optical absorbance spectra of Figure 5 can be attributed to the low-spin to high-spin state change in cytochrome a^{3+}, postulated below, during the course of the titration.) Moreover, comparison with the data of Figure 2 (inset) establishes that the increase in cytochromes a^{2+} and a_3^{2+} as determined by MCD parallels closely the increase in absorbance at 605 nm. This comparison also shows

that a significant fraction (40-50%) of the two cytochromes titrate with a potential much more positive than Cu_d^{2+} (judged by the 830 nm absorbance data of Figure 2 or the EPR data of Figure 3) while the remaining fraction has an electron affinity which is actually less than Cu_d^{2+} (see below). These data demonstrate that neither cytochrome *a* nor a_3 exhibits a single, well-defined redox potential and that attempts to fit the absorbance data of Figure 2 to a model in which, for example, cytochrome a_3 titrates with a higher potential and cytochrome *a* with a lower potential are incorrect.

Although it is now generally agreed that the *g*=3 EPR signal observed in the resting enzyme arises from low-spin cytochrome a^{3+} (2,3,6,12,21,29,34-36), there have been several suggestions as to the identity of the heme responsible for the high-spin EPR signals in the partially reduced enzyme. Under certain conditions, particularly during reoxidation of the reduced enzyme with ferricyanide or porphyrexide (28,29) or following photolysis of the a_3^{2+} · CO complex, (35-38) strong evidence exists to support the assignment of the fairly intense (representing up to 80% of the total enzyme concentration in the reoxidation experiments of Beinert et al.) rhombic high-spin component to cytochrome a_3^{3+}. The high-spin signals observed during reductive titrations of the isolated enzyme have proved to be less tractable, primarily due to their lower total concentration and to the dearth of unambiguous probes of the system under these conditions. Van Gelder and Beinert originally proposed that these species arose from cytochrome a_3^{3+}, which is antiferromagnetically coupled with Cu_u^{2+} and only becomes EPR detectable at

intermediate levels of reduction when some of the Cu_u^{2+} is reduced (6). Subsequently, Hartzell, Beinert, and Hansen (28,30,34) suggested that this species is due to cytochrome a^{3+} which exhibits the low-spin signal at g=3 in the oxidized enzyme but undergoes a low-spin to high-spin transition at intermediate levels of reduction to become EPR active as a g=6 species. Wilson and Leigh (26) originally identified the g=6 species with cytochrome a^{3+} but recently Wilson et al. (27) have indicated that an assignment of the high-spin intermediate to either cytochrome a_3^{3+} or a^{3+} is consistent with their data. A comparison of our EPR (Figure 4) and MCD data (Figures 5 and 6) allows an assignment of the high-spin species. If cytochrome a_3^{3+} were responsible for the g=6 species, then all of the cytochrome a would be accounted for by the sum {[a^{3+}] as measured by the g=3 EPR signal plus [a^{2+}] determined from the MCD data}. Alternatively if the g=6 species also arise from cytochrome a^{3+} then the total cytochrome a would be obtained as the sum {g=6 species plus g=3 species plus [a^{2+}] as measured by the MCD data}. These two alternative quantities are plotted in Figure 7 as a function of the degree of reduction of the enzyme. The comparison shows clearly that the second hypothesis, requiring that cytochrome a^{3+} appears as g=6 species at intermediate levels of reduction, is significantly more consistent with the data. The obvious conclusion from these data is that during anaerobic reduction of cytochrome oxidase a fraction of the cytochrome a undergoes a low-spin to high-spin state change.

A possible difficulty with a direct comparison of MCD and

EPR data is that the two techniques employ very different experimental conditions for routine data acquisition; the MCD experiments were conducted at 11°C with a heme concentration of 10 μM, whereas the EPR data are obtained at 12°K at a heme concentration of 110 μM. Therefore two obvious sources of error may result, one from the difference in measurement temperature, the other from the difference in protein concentration. However, both MCD and magnetic susceptibility measurements (3,5) eliminate the possibility of temperature dependent spin-state changes in the oxidase. We have attempted to assess the effects of concentration differences by comparing optical data from the MCD and EPR titrations. Normalized absorbance changes at 443 nm were plotted versus normalized absorbance changes at 420 nm. Absorbance data from the MCD and EPR titrations fell on the same curve in this plot and suggest that there is no concentration induced alteration of the titration behavior under these two sets of conditions.

Carbon Monoxide Mixed-Valence Cytochrome Oxidase

The data of Figure 6 establish that the redox potentials of cytochromes a and a_3 are similar. However, following the initial observations of Wharton and Tzagoloff (39,40), Greenwood and coworkers (41) and Wilson and Lindsay (42,43) have shown that in the presence of carbon monoxide a species of cytochrome oxidase is formed which contains reduced cytochrome a_3^{2+} as its CO complex while cytochrome a remains in its oxidized state, the

so-called mixed-valence compound. The formation of this species has been attributed to an increase in the redox potential in cytochrome a_3 induced by the much higher affinity of CO for a_3^{2+} than for a_3^{3+}. Furthermore the dependence for the redox potential with CO concentration is 30 mV for each ten-fold increase in the carbon monoxide concentration, and, at high CO concentrations, the CO binding species titrates with an n value of 2. These data were interpreted in terms of a model in which CO binds only to oxidase molecules in which both cytochrome a_3 and the EPR undetectable copper are reduced (42,43). An alternative model in which only cytochrome a_3 is reduced in the CO mixed valence species has also been proposed (41,44).

We have investigated the mixed-valence CO compound optically, by EPR and by MCD. The mixed-valence species can be obtained by several techniques, the simplest being either incubation of the oxidized enzyme under a CO atmosphere or oxidation of the fully reduced CO complexed enzyme with excess ferricyanide. Both techniques as well as preparation by reductive titration (see below) yield the mixed-valence complex with spectral properties as shown in Figure 8. The corresponding spectra for the oxidized enzyme and fully reduced cytochrome oxidase in the presence of CO are also shown for comparison. The optical spectrum exhibits the peak at 428 nm characteristic of the complex (41), significantly blue-shifted with respect to the 418-422 nm peak of the oxidized enzyme. The EPR spectrum of the mixed-valence complex, both in the low-field region characteristic of high- and low-spin heme iron and in the g=2, Cu_d^{2+}, region is identical to

that exhibited by oxidized enzyme except for a slight high-spin (g=6) signal. Quantitation of the high-spin signal shows that this corresponds to less than 0.02 moles g=6 species per mole of oxidase. Significant in the comparison of the mixed-valence and oxidized enzyme EPR spectra is the fact that no new species are detected in the mixed-valence species. This is consistent with the hypothesis of Wilson and Lindsay (42,43) that CO binding requires reduction of both cytochrome a_3 and the EPR undetectable copper of the enzyme. Were the mixed-valence enzyme to contain only one electron (41,44), it being present in the $a_3^{2+} \cdot$ CO complex, one would anticipate the appearance of a new EPR resonance appropriate to Cu_u^{2+} since the antiferromagnetic coupling between a_3^{3+} and Cu_u^{2+} would have been broken by reduction of cytochrome a_3. Wever et al. (36) have recently reported EPR results similar to these presented here, i.e., that the EPR spectrum of the mixed valence species is indistinguishable from that exhibited by the resting enzyme.

The MCD spectrum of the CO mixed-valence species (Figure 8) is very similar to that exhibited by the oxidized enzyme. Previously, we have shown that the MCD spectrum of the oxidized enzyme is dominated by the cytochrome a^{3+} contribution and had deduced that the MCD intensity of the $a_3^{2+} \cdot$ CO complex is very weak (3). Therefore, we expect, and observe, that the MCD spectrum of oxidized enzyme ($a^{3+}a_3^{3+}$) and of the CO mixed-valence enzyme ($a^{3+}a_3^{2+} \cdot$ CO) are very similar. The slightly greater intensity at the 435 nm trough for the mixed valence complex

corresponds to the weak MCD *A* term contribution (442 nm peak, 428 nm crossover, 434 nm trough) of the $a_3^{2+} \cdot CO$ complex (see Figure 4) (3). The MCD peak at 452 nm ($\frac{\Delta\epsilon}{Tesla} = 2$) arises from a slight amount (<6%) of reduced cytochrome *a* in this preparation of the CO mixed-valence compound (vide supra). The MCD spectrum of the fully reduced enzyme CO complex (Figure 7) i.e., with cytochrome *a* completely reduced, has correspondingly greater intensity in this region ($\frac{\Delta\epsilon}{T}$ (452 nm) = 35) as we have shown previously (3). Moreover, in the presence of CO, cytochrome a^{2+} is the only species to have MCD intensity at wavelengths longer than 450 nm so that the ratio of the MCD intensity at 452 nm of a given sample to that at 452 nm exhibited by the fully reduced enzyme CO complex provides a direct measure of the amount of reduced cytochrome *a* in the sample. We* have observed that the degree of oxidase reduction observed in preparations of the mixed-valence oxidase by incubation with carbon monoxide can exceed 50%; indeed in preparations with significant contamination with cytochromes b-c_1, 100% reduction of the enzyme can be obtained. Such over-reduction appears to have occurred with the sample of mixed-valence oxidase previously used for MCD by Greenwood et al. (45). Their published spectrum has a substantial contribution from a peak at 452 nm and using the criteria just described, we calculate that their sample had the composition 40% $a^{2+} \cdot a_3^{2+} \cdot CO$ plus 60% $a^{3+} \cdot a_3^{2+} \cdot CO$. They subsequently observed that low-temperature photolysis failed to elicit

---

*T. Antalis and G. Palmer, unpublished.

the low-spin a^{3+} MCD *C* term at 420 nm. Greenwood et al. (45) used this observation to conclude that the transition of low-spin a_3^{2+} to high-spin a_3^{2+} produced by photolyzing away the carbon monoxide was accompanied by a parallel low-spin to high-spin state change in cytochrome a^{3+}. However, this result is more plausibly explained by recognizing that a sizable fraction of cytochrome *a* was reduced prior to photolysis. Analogous experiments performed by Beinert and Shaw using EPR spectroscopy reveal that no more than 15% of the enzyme contributes a high-spin signal after photolysis (29) and this they attribute to cytochrome a_3^{3+} not to cytochrome a^{3+}.

Reductive Titrations of Cytochrome Oxidase Under a Carbon Monoxide Atmosphere

We have investigated the relationship between carbon monoxide binding shifts in heme *a* midpoint potentials in more detail by carrying out reductive titrations of the enzyme under a carbon monoxide atmosphere. A difficulty with this experiment, as implied above, is the autoreduction of cytochrome oxidase to form the CO mixed-valence species. This is seen in the optical data, obtained during a combined EPR/optical titration, shown in Figure 9. The absorbance change at 432 nm, indicative of $a_3^{2+} \cdot$ CO complex formation (36), is roughly 50% complete prior to external electron addition. Complete formation of the mixed-valence CO complex under a CO atmosphere generally requires several hours (41). For the data of Figure 9 the first point

was obtained approximately 30 minutes after anaerobiosis and consequently only partial formation of the mixed-valence complex has occurred. The formation of the a_3^{2+} · CO complex is subsequently completed by dithionite addition before either the EPR detectable copper (judged by the 830 nm band) or cytochrome *a* (absorbance change at 605 nm) is reduced. The latter two species subsequently titrate in the second half of the titration. From these data, we calculate that the redox potential for cytochrome a^{3+} is 45 mV more positive than that of the EPR detectable copper in the presence of CO.

Figure 10 shows the corresponding MCD spectra obtained during a reductive titration of the enzyme under a CO atmosphere (spectra 2-8) as well as the MCD spectrum of the resting aerobic enzyme (spectrum 1). Spectrum 2 was recorded after anaerobiosis under CO but prior to addition of dithionite. The formation of the mixed valence species is apparent in this spectrum as the increase in trough intensity at 434 nm ($\frac{\Delta\varepsilon}{\text{Tesla}} = -21.5$) compared to the aerobic enzyme ($\frac{\Delta\varepsilon}{\text{Tesla}}$ (434 nm) = -18.7). Optical spectra, recorded immediately following each MCD spectrum, showed that the absorbance increase at 432 nm is maximal following spectrum 3 of Figure 9 indicating complete formation of the a_3^{2+} · CO complex. In agreement with the optical data of Figure 9, appreciable reduction of cytochrome *a*, corresponding to an increase in MCD intensity at 452 nm, does not occur until the CO complex of cytochrome a_3^{2+} is completely formed. It should be pointed out that this conclusion corresponds to the equilibrium situation: we have noticed in the course of these experiments that prior to complete

formation of a_3^{2+} · CO addition of reducing equivalents results in a transient increase in cytochrome a^{2+} concentration (judged either by an increase in absorbance at 605 nm or at 443 nm) but with time cytochrome a is reoxidized and concurrently the cytochrome a_3^{2+} · CO species is formed.

Figure 11 summarizes MCD, EPR, and optical data obtained during reductive titrations of cytochrome oxidase under a CO atmosphere. The EPR data show little decrease in the g=3 low-spin concentration until complete formation of the a_3^{2+} · CO complex. The appearance of reduced cytochrome a (452 nm MCD peak) is likewise delayed until a_3^{2+} · CO is formed. The subsequent disappearance of cytochrome a^{3+}, judged by the decrease in the g=3 signal, parallels the appearance of cytochrome a^{2+}. Throughout the titration the g=6 high-spin concentration remains low, never exceeding more than 0.05 spins per oxidase molecule. The decrease in the g=2 Cu_d^{2+} EPR signal lags the titration of the g=3 signal; fitting the data to a Nernst equation expression shows that the difference in potentials for these two species ($E_{m_{7.4}}$ (g=3) - $E_{m_{7.4}}$ (g=2)) is 45 mV, in agreement with the difference in potential for the two metals calculated from the absorbance data (Figure 9).

DISCUSSION

MCD is unique among the techniques which have been applied to the study of cytochrome oxidase in that it provides direct information on the individual concentration of reduced cytochromes

a and a_3 during reductive titrations. Neither the EPR spectra nor the absorbance changes observed under analogous conditions provide this information unambiguously. The data from an anaerobic titration of cytochrome oxidase under an argon atmosphere (Figure 5) show that approximately equal amounts of reduced cytochromes a and a_3 are produced upon addition of reductant and that this relationship holds throughout the course of the titration. This finding explains the observation, often made in the past (23-25,46) and documented here in Figure 2, that the absorbance increase at 605 nm is essentially linear with reductant added during reductive titration of cytochrome oxidase. This behavior reflects the appearance of approximately equal amounts of both of the reduced cytochromes at each point in the titration and not, as has been proposed (11,47,48), equal extinction coefficients at 605 nm for the two reduced cytochromes. The assumption of equal extinction coefficients and divergent redox potentials for cytochromes a and a_3 was invoked to account for biphasic Nernst plots obtained during potentiometric titrations of both submitochondrial particles and purified cytochrome oxidase and had formed the basis for the spectral heme-heme interaction model. The apparent increase in extinction coefficient for cytochrome a^{2+} upon binding of CO by cytochrome a_3^{2+} was explained as a manifestation of this type of interaction. The data from Figures 5 and 11 show that a more plausible explanation for these observations maintains the extinction coefficient for cytochrome a^{2+} at the same value (3,13-15, 49-52), regardless of the spin or valence state of cytochrome a_3, and allows

the redox potential of cytochrome *a* to vary as redox or ligand changes occur at a_3; the linkage between the two hemes clearly affects the affinity constant of a_3 for ligands (including the electron) which is dependent upon the redox status of cytochrome *a* (13).

Van Gelder et al. (25,48) have reported anaerobic reductive and potentiometric titration data in which the midpoint potentials of cytochromes *a* and a_3 are approximately equal at 280 mV. In this system the EPR detectable copper, responsible for the 830 nm band, was also assigned a midpoint potential of 280 mV. The results we present here are distinctly different from these. This can be seen most clearly by comparing either the optical data at 830 nm (Figure 2) or the EPR data at g=2 (Figure 3) with the MCD data of Figure 5. In the initial stages of the titration (less than 1 e^-/oxidase added) there is almost no decrease in the concentration of Cu_d^{2+} while in the same range both cytochromes *a* and a_3 show appreciable reduction. During this part of the titration the redox potentials of the cytochromes are clearly more positive than that exhibited by Cu_d^{2+}. In the later stages of the titration, the Cu_d^{2+} titrates with a slightly more positive potential than do the hemes. Using the data of Figure 2 and assuming, in accord with the MCD data of Figure 5, that at 2 e^-/oxidase 50% of the total cytochrome *a* and 50% of the total cytochrome a_3 are reduced, we calculate that the cytochromes *a* and a_3 that titrate in the first half of the titration do so with a potential 100 mV more positive than Cu_d^{2+}. The cytochromes *a* and a_3 which titrate during the second half of

the titration do so with a potential 35 mV more negative than that of Cu_d^{2+}. The deconvoluted data (taken from Figure 2) used in these calculations are shown in Figure 12. If the midpoint potential for Cu_d^{2+} is taken as 250 mV (27) then the cytochromes a and a_3 which titrate in the first half of the titration have a midpoint potential of 350 mV, while those titrating in the second half of the titration have a midpoint potential of 215 mV. Similar midpoint potential values, albeit with a different interpretation, have been obtained by Wilson and coworkers (26) and Van Gelder and coworkers (48) for the 50% change in 605 nm absorbance increase which titrates with a high redox potential (340-380 mV) and the subsequent 50% increase in 605 nm absorbance which titrates with a lower midpoint potential (200-240 mV). The data presented here and particularly the MCD data of Figure 5 which led to the analysis of Figure 12 provide evidence for heme/heme interaction via redox potential. This model, which has been discussed by several research groups (12-15), can be summarized by scheme (1):

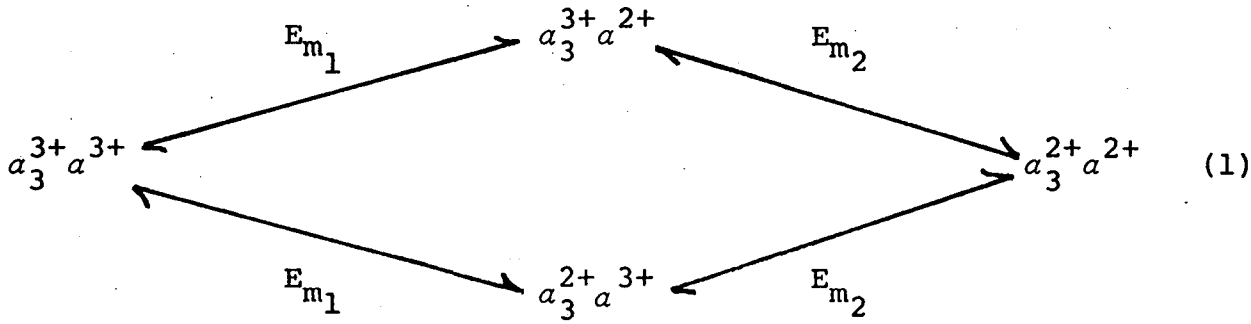

(1)

where E_{m_1} represents the redox potential for the reduction of the $a_3^{3+}a^{3+}$ species, and E_{m_2} represents the redox potential for

the reduction of the intermediate species $a_3^{2+}a^{3+}$ and $a_3^{3+}a^{2+}$. Our data show that $E_{m_1} > E_{m_2}$ which indicates negative cooperativity in cytochrome oxidase, i.e., in the oxidized enzyme the reduction of either a^{3+} or a_3^{3+} is equally probable, however, once either cytochrome is reduced subsequent reduction of the other cytochrome is more difficult. In this scheme the contributions of cytochromes a and a_3 to the absorbance changes at 605 nm are actually irrelevant, the sigmoidal Minneart plots (9) being a consequence of the equivalence and linkage in the potentials of the two cytochromes. However the combination of this behavior together with the traditional estimates (1) for the relative contributions of a and a_3 to the change in absorbance at 605 nm (85% and 15% respectively) nicely explains the apparent changes in extinction coefficient observed by Wilson et al. (11) during potentiometric titrations in the presence of carbon monoxide and azide. The very high affinity of CO for a_3^{2+} confines scheme 1 to the lower pathway; thus, the large (ca. 85%) extinction changes are observed during the second (more negative) stage of reduction. On the other hand azide has a high affinity for a_3^{3+} thus confining scheme 1 to the upper pathway and the large extinction changes are seen in the first (more positive) stage of reduction. This behavior is qualitatively and quantitatively that observed by Wilson et al. (11,26,27,53).

The interesting oxidative titrations of cytochrome oxidase reported by Schroedl and Hartzell (54) are also explained by scheme 1. They showed that during reoxidation with either ferricyanide or 1,1'-bis (hydroxymethyl) ferricinium cation

a low potential heme, accounting for roughly 80-85% of the absorbance change at 605 nm, was oxidized in the initial stages of the titration, followed by a second, higher potential heme which accounted for the remaining 15-20% of the absorbance change. They attributed the low potential heme to cytochrome *a* in agreement with our assignment here of cytochrome *a* to the principal absorbing species at 605 nm. Under the conditions of their experiments it appears as if the reoxidation of reduced oxidase proceeds exclusively along the lower pathway from right to left in scheme 1.

The two hemes of cytochrome oxidase appear to be physically distant from each other in the protein (see, for example, Ref. 55,56) so that the mechanism by which the negative cooperativity observed during reductive titrations is exerted should be more complex than a simple electrostatic interaction between the two hemes. The g=6 species observed during the titration provides insight into a possible mechanism. In the resting enzyme the g=3 low-spin EPR signal accounts for one heme per oxidase which we take to be associated with cytochrome a^{3+} (6,21,36). During a reductive titration, however, the g=3 signal disappears more rapidly than cytochrome a^{2+} appears (Figure 7). This discrepancy can be understood by postulating that the g=6 signal arises from cytochrome a^{3+} which undergoes a g=3 → g=6 spin state transition during the titration. The g=6 signal is maximal at half-reduction of the enzyme, i.e., when, as postulated in scheme (1), the concentration of the intermediate species, $a^{3+}a_3^{2+}$ and $a_3^{2+}a^{3+}$ are maximal. This observation suggests that the reduction of

cytochrome a_3 in enzyme molecules in which cytochrome a remains oxidized triggers the change in ligand configuration which lowers the reduction potential of cytochrome a^{3+} and simultaneously generates the g=6 signal.

The correlation between cytochrome a^{3+} and the high-spin species developed in Figure 7 argues that both the axial and rhombic components originate from cytochrome a^{3+} under reductive titration conditions. Beinert and Hartzell (34) have reached a similar conclusion based on combined reflectance spectroscopy and EPR measurements. An alternate hypothesis has been suggested in which the axial and rhombic components of the g=6 signal originate from cytochromes a^{3+} and a_3^{3+} in the half reduced intermediate of Equation 1 (15). Axial and rhombic high-spin EPR signals have been observed under conditions other than reductive or redox titration, notably by photodissociation of the CO complex of partially reduced enzyme (31,35,57) and during reoxidation of the reduced protein with ferricyanide or porphyrexide (28,29). The photodissociation experiments were carried out at either 10°K (31) or 77°K (35) and in both cases resulted in an increase in the intensity of a rhombic g=6 species. The most plausible explanation for these low temperature results requires photodissociation of CO from cytochrome a_3^{2+} followed by oxidation to a_3^{3+} and concomitant reduction of cytochrome a. This interpretation assigns the rhombic high-spin species to cytochrome a_3^{3+} under these circumstances. Beinert and Shaw (29) have attributed the intense, rhombic g=6 signal observed during reoxidation of the reduced enzyme with ferricyanide or porphyrexide to cytochrome

a_3^{3+}. However, as pointed out by these authors there are differences in the size of the rhombic splittings observed under different experimental conditions so that, a priori, there is no reason to expect that in all experiments in which a rhombic g=6 species is observed that the species responsible is cytochrome a_3^{3+}. Thus our tentative assignment of both axial and rhombic components of the g=6 species to cytochrome a^{3+} is not contradicted by these results. However the concentration of the rhombic component in our experiments is low enough and the inaccuracy of our EPR quantitations high enough that we cannot conclusively make these assignments. A study of the pH dependence of our titration results may provide further insight into the assignment of the rhombic g=6 species since Hartzell and Beinert (28,30) have shown that the appearance of the signals is markedly dependent on pH: at low pH ($\sim$6) the g=6 signal is reported to be more intense than that observed at pH 7.4 whereas at higher pH ($\sim$9.3) less than 0.1 g=6 spins are observed per oxidase molecule. What is clear from our present results, however, is that a sizeable fraction of the g=6 species does arise from cytochrome a^{3+}. A corollary to this conclusion is that the pair, cytochrome $a_3 \cdot Cu_u$, are tightly coupled in their redox properties so that the intermediate states, $a_3^{2+} \cdot Cu_u^{2+}$ and $a_3^{3+} \cdot Cu_u^{1+}$, which would be expected to show EPR signals from Cu_u^{2+} and a_3^{3+} respectively do not occur in measurable quantities.

In the presence of CO the interaction mechanism between cytochromes a and a_3 is dramatically altered. Our data indicate that in the half-reduced complex, obtained either as the "mixed-

valence" oxidase or by titration, both cytochrome a_3 and a second component, the EPR undetectable copper, are reduced and cytochrome a and the EPR detectable copper are maintained in the oxidized form. These observations are consistent with experiments performed by Wilson, Lindsay and coworkers (42,43), and the recent results obtained by Wever et al. (36). Moreover, the EPR reductive titration data (Figure 10) show that at partial formation of the mixed-valence CO complex there are no new EPR species detectable. This supports the observation that ($a_3^{3+} \cdot Cu_u^{2+}$) titrates as a two electron acceptor in the presence of high concentrations of CO (42). We note that our data were obtained in the high CO concentration limit (43) and that a different result may be obtained upon lowering the carbon monoxide concentration. Following formation of the $Cu_u^{1+}a_3^{2+} \cdot$ CO complex, cytochrome a^{3+} and Cu_d^{2+} titrate as one electron acceptors with a difference in potential of 45 mV. These values are in good agreement with the data of Wilson and Leigh (26) for the difference in midpoint potentials for cytochrome a and the EPR detectable copper (E_m (a^{3+}) = 265 mV, E_m (Cu_d^{2+}) = 225 mV, ΔE_m = 40 mV) under similar conditions. The Nernstian behavior of the g=3 species (cytochrome a^{3+}) in the presence of CO is in marked contrast to that observed under argon as is the absence of significant amounts of g=6 species during a CO titration. Taken together these observations suggest that the binding of CO to a_3^{2+} forces the normal potential modifying heme-heme interaction into the lower pathway of scheme 1, as discussed above. The lack of g=6 signals in the presence of carbon monoxide is, at first sight, surprising

for at half reduction the species $a^{3+}a_3^{2+} \cdot CO$ is present at about 100% yield. As the MCD spectra clearly show cytochrome a is ferric low-spin at this point, we are forced to postulate that the trigger for the spin-state change in cytochrome a^{3+} observed in the absence of ligands is the production of high-spin ferrous cytochrome a_3^{2+}.

Preliminary titration results obtained for cytochrome oxidase in the presence of the inhibitors azide and formate and monitored by both MCD and EPR show similar results: the heme-heme interaction mechanism observed under an inert atmosphere is interrupted (Palmer, G., Garcia-Iniguez, L., Babcock, G., and Vickery, L., in preparation). Contrary to the CO case these inhibitors stabilize cytochrome a_3^{3+} and reduction of cytochrome a^{3+} occurs in the first half of the titration. Beinert and Van Gelder (6), using EPR, reported similar behavior during a titration of cytochrome oxidase in the presence of azide. The g=3, cytochrome a^{3+} EPR signal titrated in the first half of the titration and at half reduction a g=2.9 signal, which they attribute to the cytochrome $a_3^{3+} \cdot N_3^-$ complex, was maximal. Wilson and coworkers (26) performed redox titrations with N_3^- present and reported, in agreement with our results mentioned above and those of Beinert and Van Gelder (6), that the g=3 species titrates as a high potential species and the g=2.9 species titrates with a much lower potential. However, to explain these results in the context of their spectral heme-heme interaction model they attribute the g=3 species to cytochrome a_3^{3+} and the g=2.9 species to cytochrome $a^{3+} \cdot N_3^-$. Our MCD results (Ref. 3 and those quoted

above) argue strongly against this assignment since the half-reduced enzyme in the presence of azide exhibits the 452 nm MCD absorption characteristic of cytochrome a^{2+}.

Finally we point out that the results reported here and scheme 1 apply only to the anaerobic equilibrium condition. In kinetic studies (28) it appears that cytochrome *a* is initially reduced by ferrocytochrome *c* followed by intramolecular electron redistribution within the oxidase.

Acknowledgments

This research was supported, in part, by NIH Grant GM-21337 and the Welch Foundation (C636) and, in part, by the U.S. Energy Research and Development Administration. NIH Postdoctoral Fellowship HL-02052 (to GTB) in the early stages of this research is also acknowledged. Helium was supplied by the Office of Naval Research.

Abbreviations: EPR, electron paramagnetic resonance; MCD, magnetic circular dichroism.

Table I: Spectral Parameters Cytochromes a and a_3 Used in the Analysis of MCD Data.

	Cytochrome a^{2+}	Cytochrome a_3^{2+}
$\frac{\Delta\varepsilon}{\text{Tesla}}$ (446.7 nm)	0	79.3
$\frac{\Delta\varepsilon}{\text{Tesla}}$ (452.0 nm)	35.0	10.7
$\frac{\Delta\varepsilon}{\text{Tesla}}$ (455.0 nm)	27.5	0

At each point in the titration $[a_3^{2+}]$ and $[a^{2+}]$ were determined from the MCD intensities at 446.7 nm and 455 nm, respectively. As a check on the validity of these determinations, we then used these $[a_3^{2+}]$ and $[a^{2+}]$ to calculate the MCD intensity at 452 nm. Agreement between this calculated 452 nm intensity and that observed experimentally was within 5% for the data of Figure 5.

REFERENCES

1. Lemberg, M. R. (1969) Physiol Rev. 49, 48-121.

2. Palmer, G., Babcock, G. T., and Vickery, L. E. (1976) Proc. Nat. Acad. Sci. 73, 2206-2210.

3. Babcock, G. T., Vickery, L. E. and Palmer, G. (1976), J. Biol. Chem. 251, 7907-7919.

4. Ehrenberg, A. and Yonetani, T. Y. (1961) Acta. Chem. Scand. 15, 1071-1080.

5. Tsudzuki, T. and Okunuki, K. (1971), J. Biochem. 69, 909-922.

6. Van Gelder, B. F. and Beinert, H. (1969) Biochim. Biophys. Acta., 189, 1-24.

7. Lang. G., Lippard, S. J. and Rosen, S. (1974) Biochim. Biophys. Acta. 336, 6-14.

8. Falk, K. E., Vanngärd, T. and Ångstrom, J. (1977) FEBS Letts. 75, 23-27.

9. K. Minneart (1965) Biochim. Biophys. Acta, 110, 42-56.

10. Tsudzuki, T. and Wilson,D. F. (1971) Arch. Biochem. Biophys. 145, 149-154.

11. Wilson, D. F., Lindsay, J. G. and Brocklehurst, E. (1972), Biochim. Biophys. Acta. 256, 277-286.

12. Malmstrom, B. G. (1973) Quart. Rev. Biophys. 6, 389-431.

13. Nicholls, P. and Chance, B. (1974) in Molecular Mechanisms of Oxygen Activation (Hayaishi, O., ed.) pp. 479-534, Academic Press, New York.

14. Nicholls, P. and Petersen, L. C. (1974) Biochim. Biophys. Acta. 357, 462-467.

15. Wikström, M. K. F., Harmon, H. J., Ingledew, W. J. and Chance, B. (1976) FEBS Letts. 65, 259-276.

16. Hartzell, C. R. and Beinert, H. (1975) Biochim. Biophys. Acta. 368, 318-338.

17. Gibson, Q. H., Palmer, G., and Wharton, D. C. (1965) J. Biol. Chem. 240, 915-920.

18. Sutherland, J. C., Vickery, L. E., and Klein, M. P. (1974) Rev. Sci. Instrum. 45, 1089.

19. Burleigh, B. D., Jr., Foust, G. P. and Williams, C. H., Jr. (1969) Anal. Biochem. 27, 536-544.

20. Palmer, G. (1977) Anal. Biochem, in press.

21. Aasa, R., Albracht, S. P. J., Falk, K.-E., Lanne, B., and Vanngarad, T. (1976) Biochim. Biophys. Acta. 422, 260-272.

22. Smith, D. W. and Williams, R. J. P. (1970) Struct. Bonding (Berlin) Vol. 7, 1-45.

23. Van Gelder, B. F. (1966) Biochim. Biophys. Acta. 118, 36-46.

24. Mackey, L. N., Kuwana, T. and Hartzell, C. R. (1973) FEBS Letts. 36, 326-329.

25. Van Gelder, B. F., Tiesjema, R. H., Muijesers, A. O., van Buuren, K. J. H. and Wever, R. (1973) Fed. Proc. 32, 1977-1980.

26. Wilson, D. F. and Leigh, J. S., Jr. (1972) Arch. Biochem. Biophys. 150, 154-163.

27. Wilson, D. F., Erecinska, M. and Owen, C. S. (1976) Arch. Biochem. Biophys, 175, 160-172.

28. Beinert, H., Hansen, R. E. and Hartzell, C. R. (1976) Biochim. Biophys. Acta. 423, 339-355.

29. Beinert, H. and Shaw, R. W. (1977) Biochim. Biophys. Acta. (in press).

30. Hartzell, C. R. and Beinert, H. (1976) Biochim. Biophys. Acta 423, 323-338.

31. Leigh, J. S., Jr., Wilson, D. F., Owen, C. S., and King, T. E. (1974) Arch. Biochem. Biophys, 160, 476-486.

32. Vickery, L., Nozawa, T. and Sauer, K. (1976), J. Am. Chem. Soc. 98, 343-350.

33. Thomson, A. J., Brittain, T., Greenwood, C. and Springall, J. (1976) FEBS Letts. 67, 94-98.

34. Hartzell, C. R., Hansen, R. E., and Beinert, H. (1973) Proc. Nat. Acad. Sci. USA, 70, 2477-2481.

35. Wever, R., VanDrooge, J. H., VanArk, G., and Van Gelder, B. F. (1974) Biochim. Biophys. Acta. 347,215-223.

36. Wever, R., VanDrooge, J. H., Muijsers, A. O., Bakker, E. P., and Van Gelder, B. F. (1977) Eur. J. Biochem. 73, 149-154.

37. Leigh, J. S., Jr. and Wilson, D. F. (1972) Biochem. Biophys. Res. Commun. 48, 1266-1272.

38. R. Wever and B. F. Van Gelder (1974) Biochim. Biophys. Acta. 368, 311-317.

39. Wharton, D. C. (1964) Biochim. Biophys. Acta. 92, 604-611.

40. Tzagoloff, A. and Wharton, D. C. (1965) J. Biol. Chem. 240, 2628-2633.

41. Greenwood, C., Wilson, M. T. and Brunori, M. (1974) Biochem. J. 137, 205-215.

42. Lindsay, J. G. and Wilson, D. F. (1974) FEBS Letts., 48, 45-49.

43. Lindsay, J. G., Owen, C. S. and Wilson, D. F. (1975) Arch. Biochem. Biophys. 169, 492-505.

44. Anderson, J. L., Kuwana, T. and Hartzell, C. R. (1976) Biochem. 15, 3847-3855.

45. Brittain, T., Springall, Jr., Greenwood, C. and Thompson, A. J. (1976) Biochem. J. 159, 811-813.

46. Heineman, W. R., Kuwana, T. and Hartzell, C. R. (1972) Biochem. Biophys. Res. Commun. 49,1-8.

47. Wilson, D. F. and Leigh, J. S., Jr. (1974) Ann. N.Y. Acad. Sci. 227, 630-635.

48. Tiesjema, R. H., Muijsers, A. O., and Van Gelder, B. F. (1973) Biochim. Biophys. Acta. 305, 19-28.

49. Yonetani, T. (1960) J. Biol. Chem. 235, 3138-3143.

50. Horie, S. and Morrison, M. (1963) J. Biol. Chem., 238, 2859-2865.

51. Vanneste, W. H. (1966) Biochemistry 5, 838-848.

52. Gilmour, M. V., Wilson, D. F. and Lemberg, R. (1967) Biochim. Biophys. Acta. 143, 487-489.

53. Wilson, D. F. and Brocklehurst, E. S. (1973) Arch. Biochem. Biophys. 158, 200-212.

54. Schroedl, N. A. and Hartzell, C. R. (1977) Biochem. 16, 1327-1333.

55. Papa, S., Gurrieri, F. and Lorusso, M. (1974) Biochim. Biophys. Acta. 357, 181-192.

56. Yu, C. A., Yu, L. and King, T. E. (1977) Biochem. Biophys. Res. Commun. 74, 670-676.

57. Wever, R. and Van Gelder, B. F. (1974) Biochim. Biophys. Acta. 368, 311-317.

Figure Captions

Figure 1 High spin (g=6 region) ferric iron EPR signals observed for (a) 79 μM metmyoglobin fluoride and (b) a cytochrome oxidase sample, 119 μM in heme a, to which 2.34 reducing equivalents per mole of enzyme had been added. Note that the spectrum for the oxidase sample was recorded at ten fold higher instrument gain than the metmyoglobin fluoride spectrum.

Figure 2 Optical absorbance in the α band region recorded during a combined optical/EPR reductive titration of cytochrome oxidase. The sample contained 120 μM heme a initially, the optical pathlength was 2 mm. A dilution of the enzyme by approximately 5% during the course of the titration was corrected for to obtain the normalized absorbance changes, $\Delta A = \frac{A(\lambda)_{sample} - A(\lambda)_{initial}}{A(\lambda)_{final} - A(\lambda)_{initial}}$, at 605, 443 and 830 nm.

Figure 3 Quantitation of EPR resonances observed during a combined optical/EPR reductive titration of cytochrome oxidase carried out under an argon atmosphere. The oxidase preparation contained 120 μM heme a.

Figure 4 Computed MCD spectra for oxidized and reduced cytochrome a (upper) and for oxidized and reduced cytochrome a_3 (lower). Computed MCD spectra for low spin cytochrome a_3 in the oxidized (obtained as the $a_3^{3+} \cdot CN$ complex) and in the reduced (obtained as the $a_3^{2+} \cdot CO$ complex) states are also shown.

Figure 5 Soret region MCD (upper) and optical (lower) spectra of cytochrome oxidase obtained during a combined optical/MCD reductive titration. The enzyme contained, initially, 10.2 μM heme a; the optical pathlength was 1 cm. The enzyme was diluted by 3.3% during the course of the titration.

Figure 6 Quantitation of the concentrations of cytochromes $\underline{a}^{2+}$ and $\underline{a}_3^{2+}$, as a function of electrons/oxidase added, from the MCD data of the reductive titration shown in Figure 5. See text and Table I for details of the quantitation procedure.

Figure 7 Comparison of alternate models for the origin of the g=6 EPR signal observed at intermediate levels of reduction during titrations of cytochrome oxidase. The g6 signal intensity is shown (●) as well as the sums $\underline{a}^{2+}$ + g3 (◆) and $\underline{a}^{2+}$ + g3 + g6 (Δ). See text for details and conclusions.

Figure 8 Soret region optical (a) and MCD (b) spectra of oxidized ($a^{3+}a_3^{3+}$), carbon monoxide mixed valence ($a^{3+}a_3^{2+}\cdot CO$) and carbon monoxy reduced ($a^{2+}a_3^{2+}\cdot CO$) cytochrome oxidase. A sample of the oxidized enzyme, 9 μM in heme a, was incubated under a CO atmosphere (P_{CO} = 1 atm) at 4°C for eight hours to form the mixed valence species. After the spectra were recorded a few grains of solid sodium dithionite were added to achieve complete reduction of the sample. The EPR spectra (c) of oxidized

cytochrome oxidase and the carbon monoxide mixed valence species are shown in the low field (lower left panel) and in the g = 2 (lower right panel) regions. A sample of oxidized protein, 119 μM in heme a, was stoichiometrically reduced with sodium dithionite under a CO atmosphere (P_{CO} = 1 atm) and a slight excess of potassium ferricyanide was then added to form the CO mixed valence species. The optical properties of the mixed valence species formed by this technique were identical to those in (a). The spectrometer gain for the low field spectra was 8000, for the g = 2 region the gain was 3200.

Figure 9 Normalized optical absorbance changes (ΔA) observed during reductive titration of cytochrome oxidase under a carbon monoxide atmosphere (P_{CO}= 1 atm). Note partial formation of the cytochrome $a_3^{2+}\cdot CO$ complex prior to addition of reducing equivalents. To correct for this behavior the normalized ΔA values were obtained as

$$\Delta A = \frac{A(\lambda)_{\text{sample}} - A(\lambda)_{\text{aerobic enzyme}}}{A(\lambda)_{\text{final}} - A(\lambda)_{\text{aerobic enzyme}}} .$$

Figure 10 Soret region MCD spectra of aerobic cytochrome oxidase (spectrum 1) and of samples obtained at partial reduction (spectra 2-8) during a reductive titration of cytochrome oxidase, 10.1 μM in heme a, under a carbon monoxide atmosphere (P_{CO} = 1 atm).

Figure 11 Summary of optical, EPR and MCD data obtained during reductive titration of cytochrome oxidase under a carbon monoxide atmosphere (P_{CO} = 1 atm). Cytochrome $\underline{a}_3^{2+}\cdot CO$ concentrations were obtained from the optical absorbance at 432 nm (See Figure 9), cytochrome $\underline{a}^{2+}$ concentrations were obtained from the MCD intensity at 452 nm (see Figure 10). Quantitation of EPR detectable species was carried out as described in the Methods section.

Figure 12 Calculated concentrations, from Figure 2, of cytochrome $\underline{a}$ and $\underline{a}_3$ species and of the reduced form (Cu^{1+}) of the EPR detectable copper observed during reductive titration of cytochrome oxidase. The reduction of cytochromes $\underline{a}_3^{3+}$ and $\underline{a}^{3+}$ is postulated to proceed in two steps: (1) from $\underline{a}_3^{3+}\underline{a}^{3+}$, in the fully oxidized enzyme, to the intermediate half reduced state, $\underline{a}_3^{2+}\underline{a}^{3+} + \underline{a}_3^{3+}\underline{a}^{2+}$, (represented as $(\underline{aa}_3)^{5+}$) and (2) from the intermediate state to the fully reduced state, $\underline{a}_3^{2+}\underline{a}^{2+}$. See text for details.

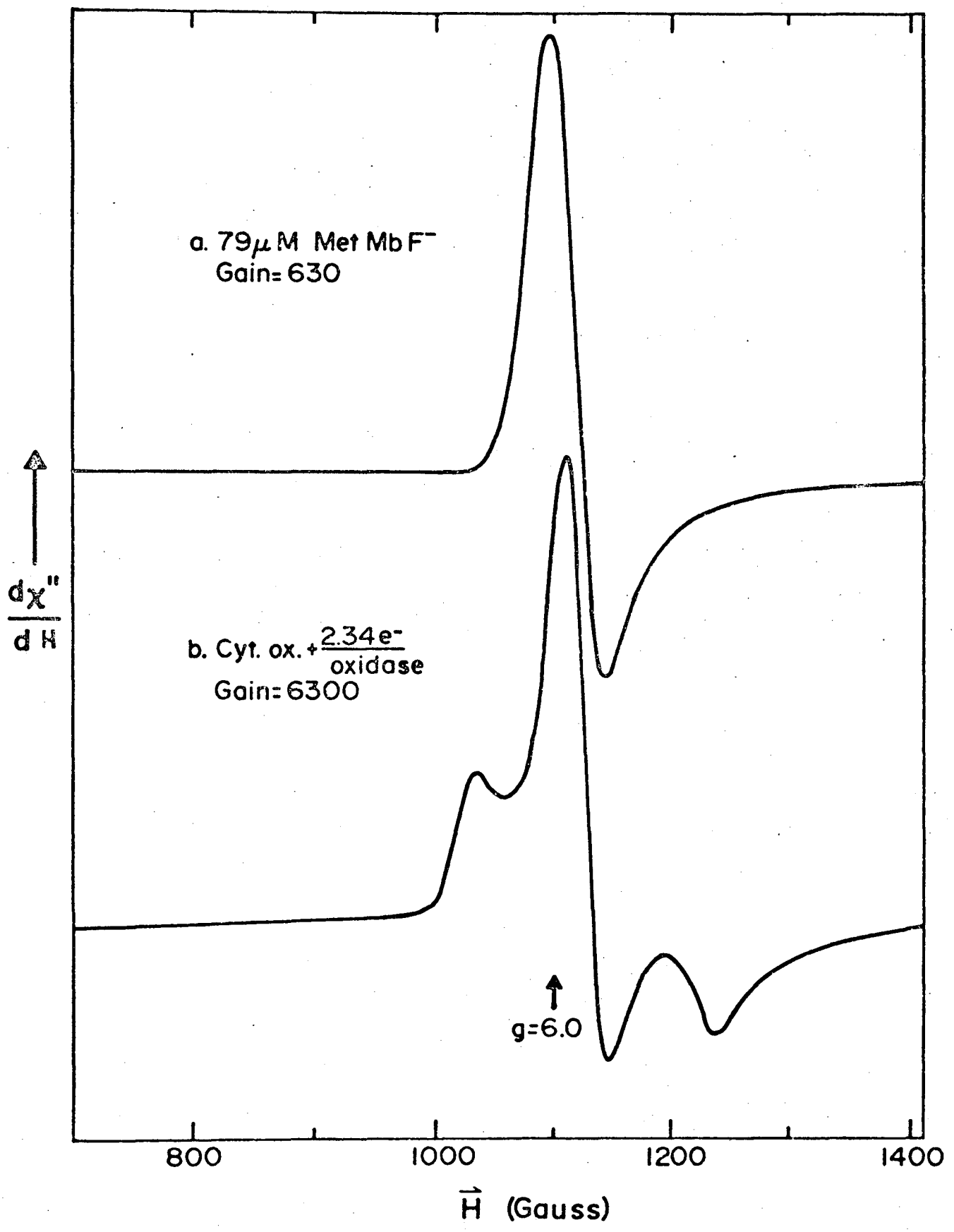
a. 79μM Met Mb F⁻
Gain=630
b. Cyt. ox. + 2.34e⁻ / oxidase
Gain=6300
g=6.0
dχ''/dH
800
1000
1200
1400
H (Gauss)

Fig. 1

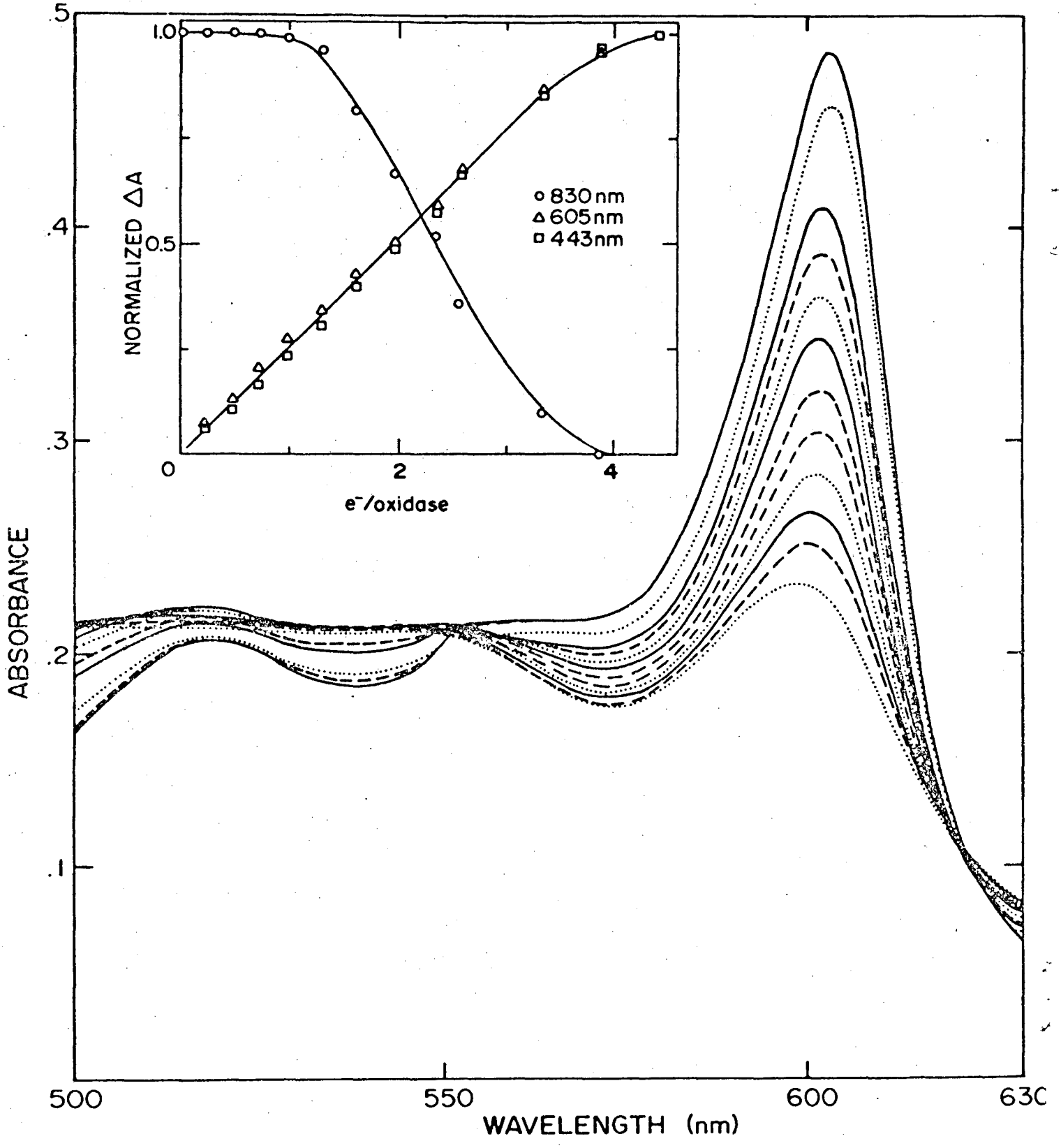
ABSORBANCE
.5
.4
.3
.2
.1
500
550
600
630
WAVELENGTH (nm)
NORMALIZED ΔA
1.0
0.5
0
2
4
e⁻/oxidase
o 830nm
Δ 605nm
□ 443nm

Fig. 2

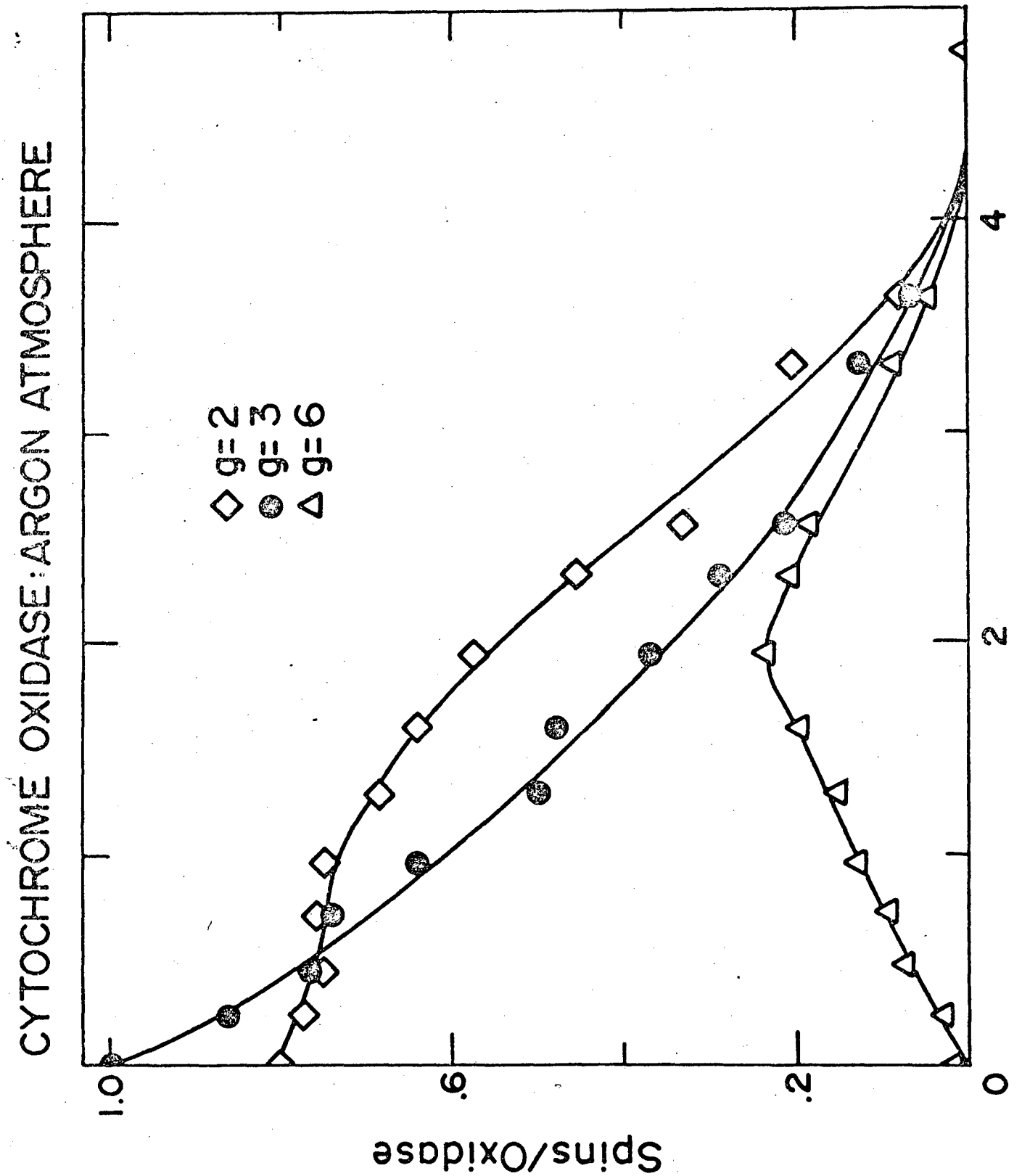
CYTOCHROME OXIDASE: ARGON ATMOSPHERE
g=2
g=3
g=6
Spins/Oxidase
1.0
.9
.2
0
2
4
e⁻/oxidase

Fig. 3

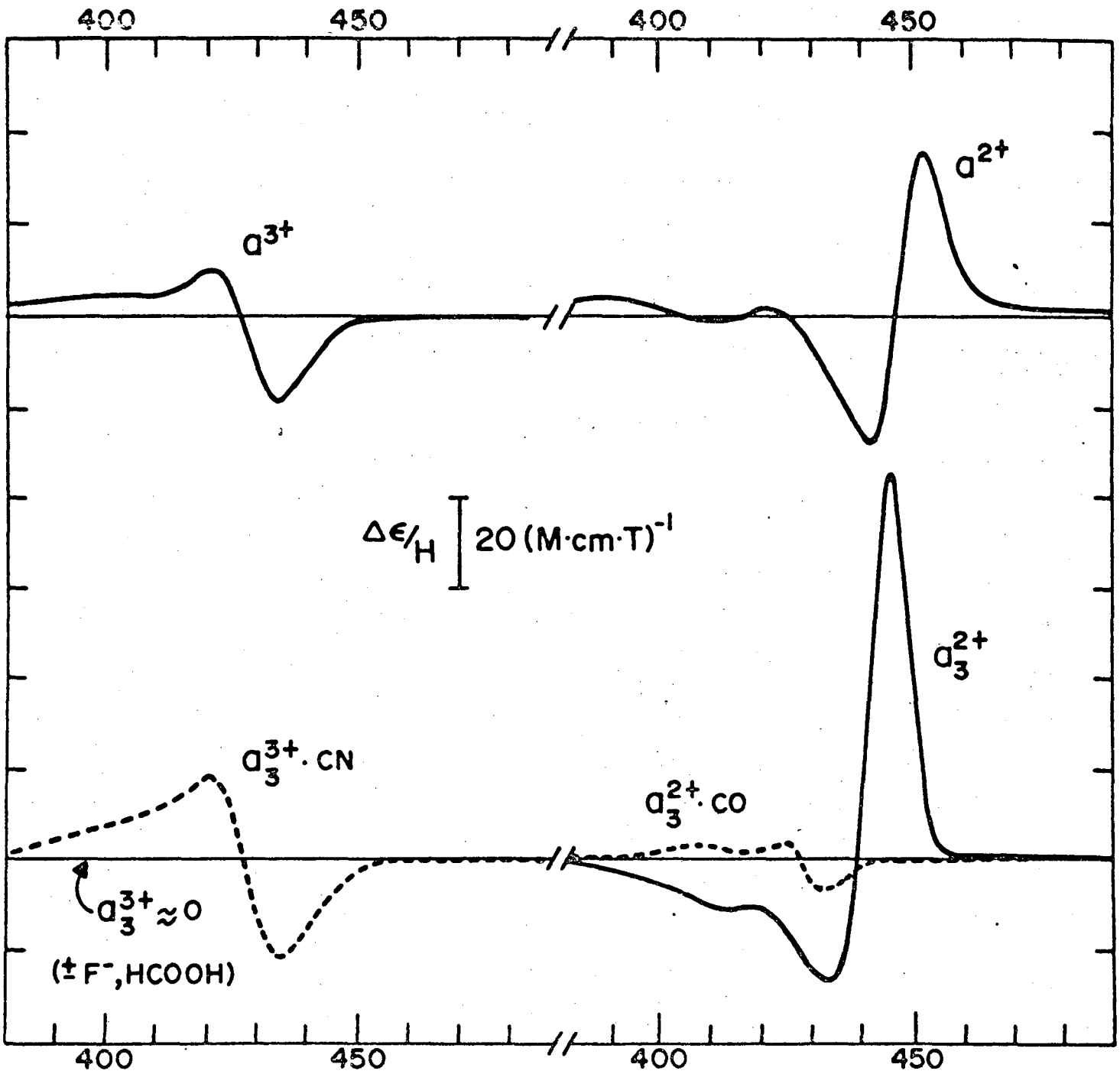
400
450
400
450
a^{2+}
a^{3+}
$\Delta\epsilon/H$ 20 $(M \cdot cm \cdot T)^{-1}$
a_3^{2+}
$a_3^{3+} \cdot CN$
$a_3^{2+} \cdot CO$
$a_3^{3+} \approx 0$
$(\pm F^-, HCOOH)$
400
450
400
450
Wavelength (nm)

Fig. 4

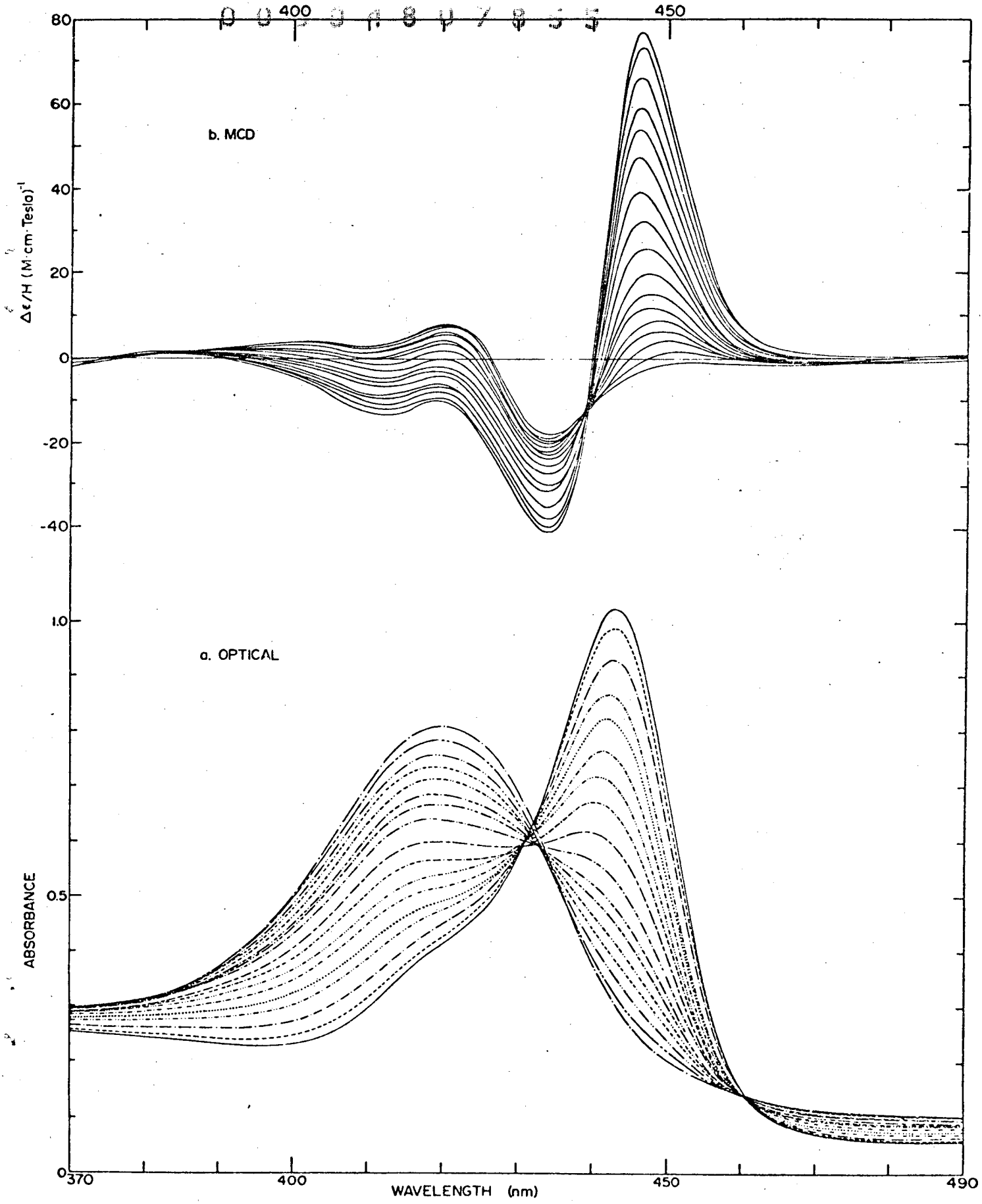
400
450
80
60
40
20
0
-20
-40
b. MCD
Δε/H (M·cm·Tesla)⁻¹
1.0
0.5
0
a. OPTICAL
ABSORBANCE
370
400
450
490
WAVELENGTH (nm)

Fig. 5

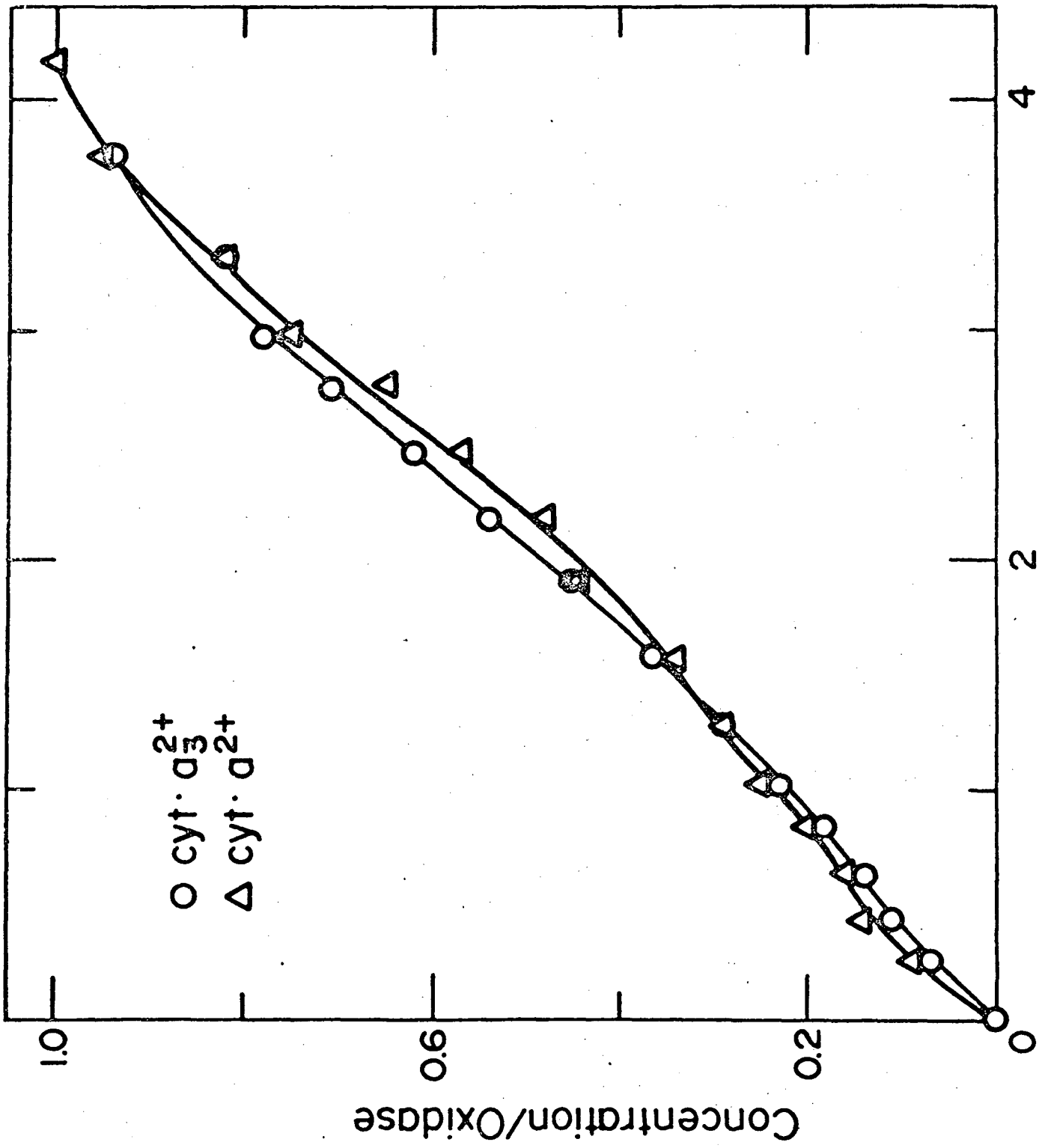

Fig. 6

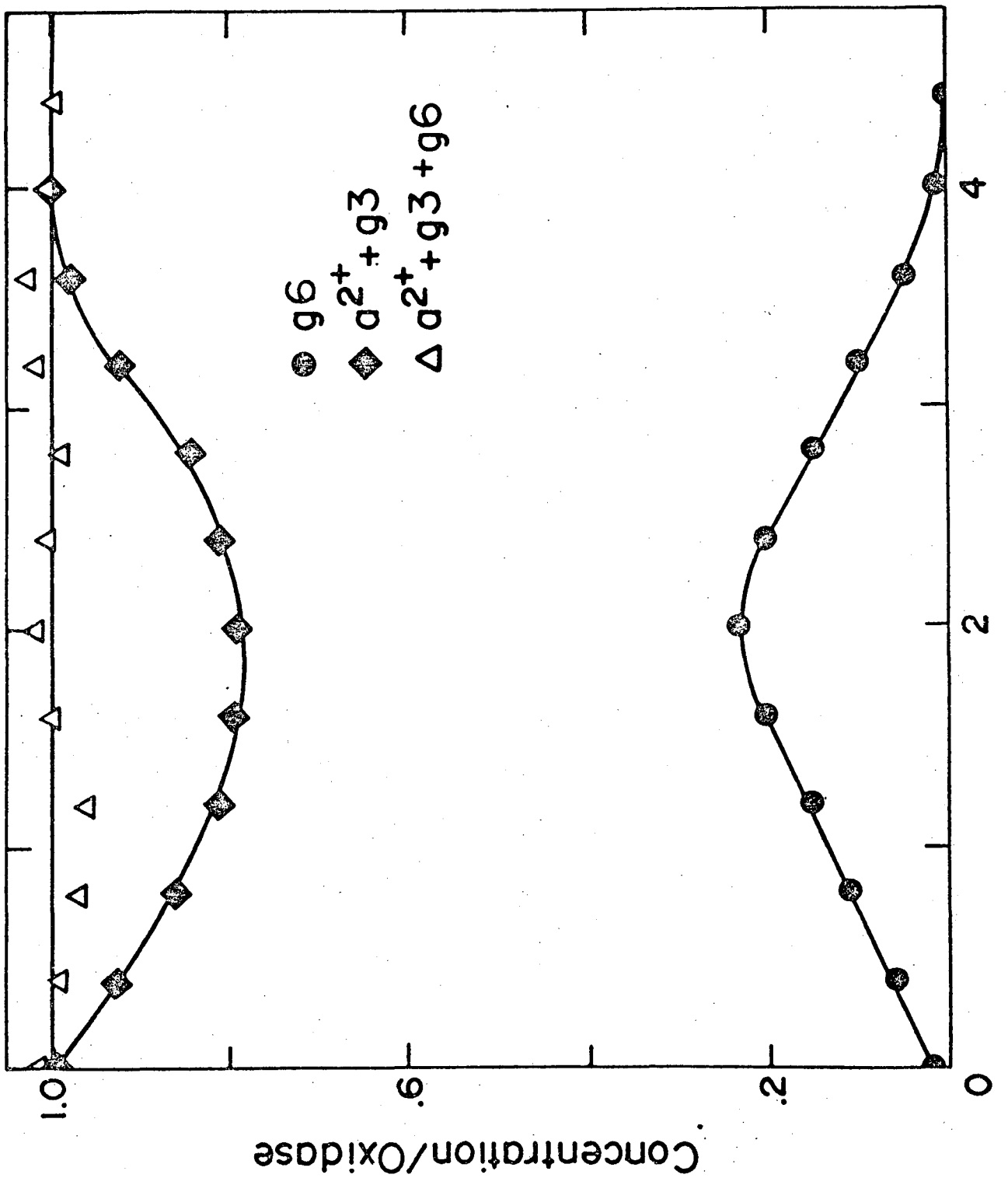

Fig. 7

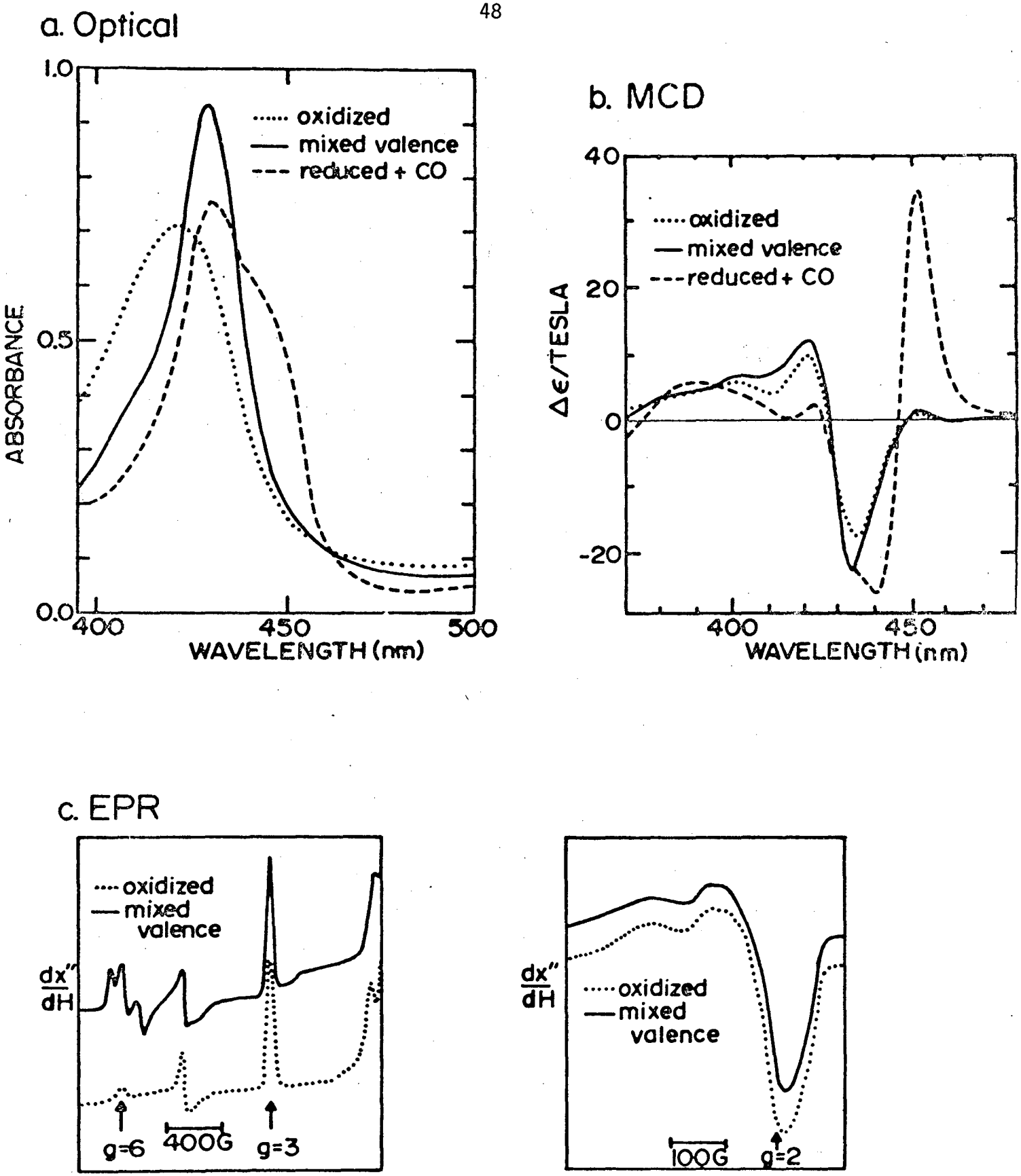
a. Optical
1.0
0.5
0.0
ABSORBANCE
400
450
500
WAVELENGTH (nm)
..... oxidized
— mixed valence
--- reduced + CO
b. MCD
40
20
0
-20
Δε/TESLA
400
450
WAVELENGTH (nm)
.....oxidized
— mixed valence
---reduced + CO
c. EPR
....oxidized
— mixed valence
dx''/dH
g=6
400G
g=3
.....oxidized
— mixed valence
dx''/dH
100G
g=2

Fig. 8

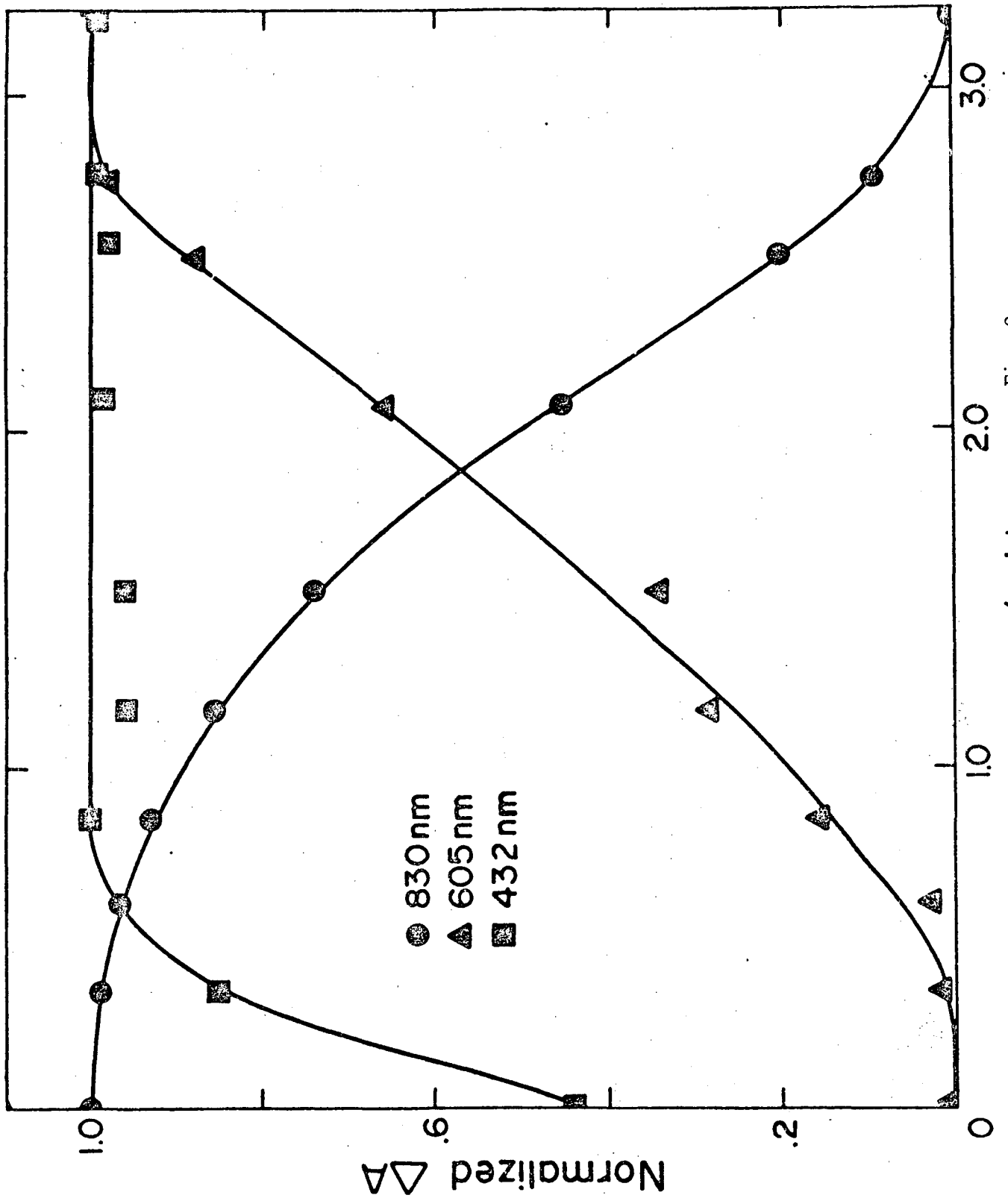

Fig. 9

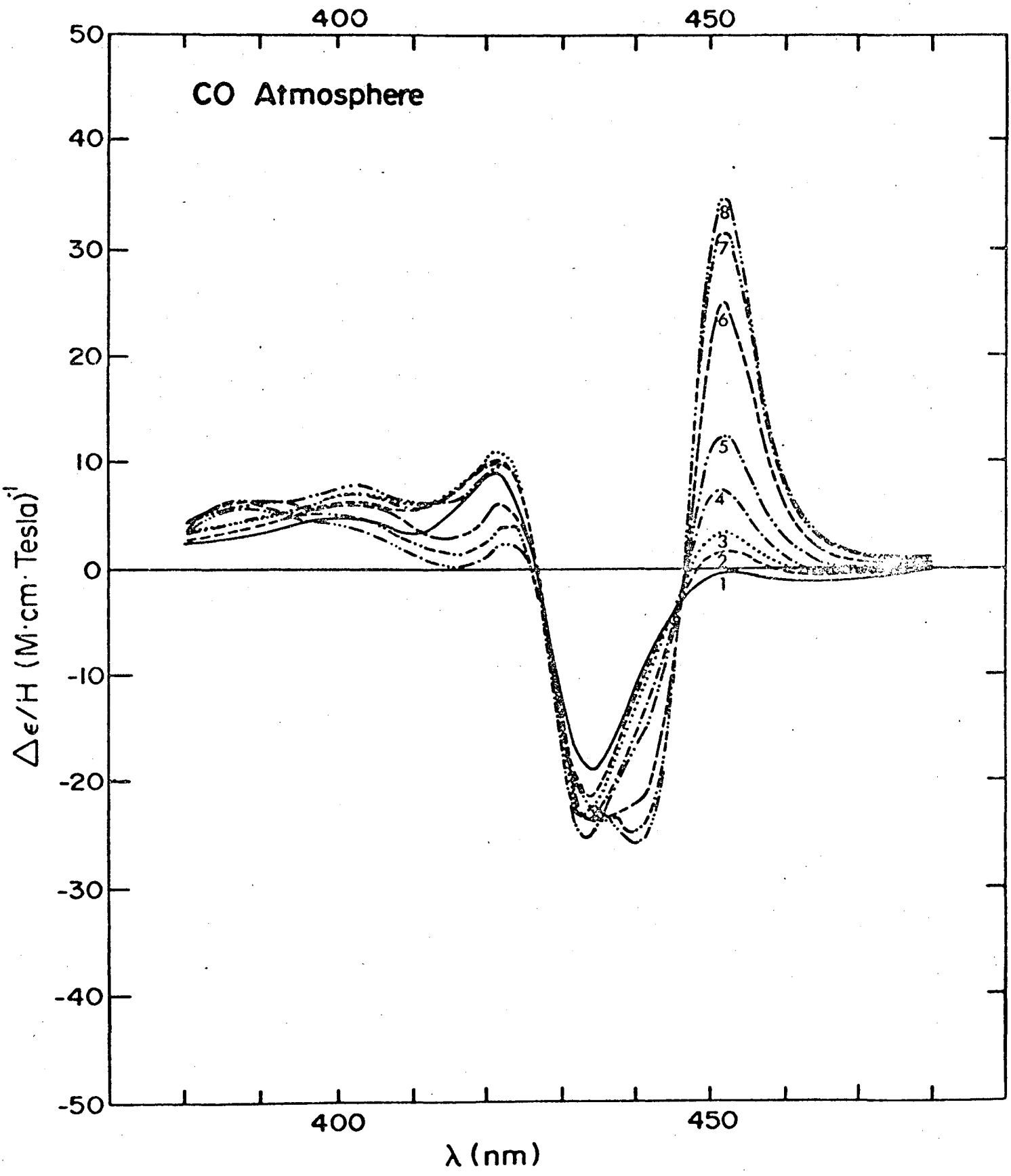
CO Atmosphere
400
450
50
40
30
20
10
0
-10
-20
-30
-40
-50
Δε/H (M·cm·Tesla)⁻¹
λ (nm)
1
2
3
4
5
6
7
8

Fig. 10

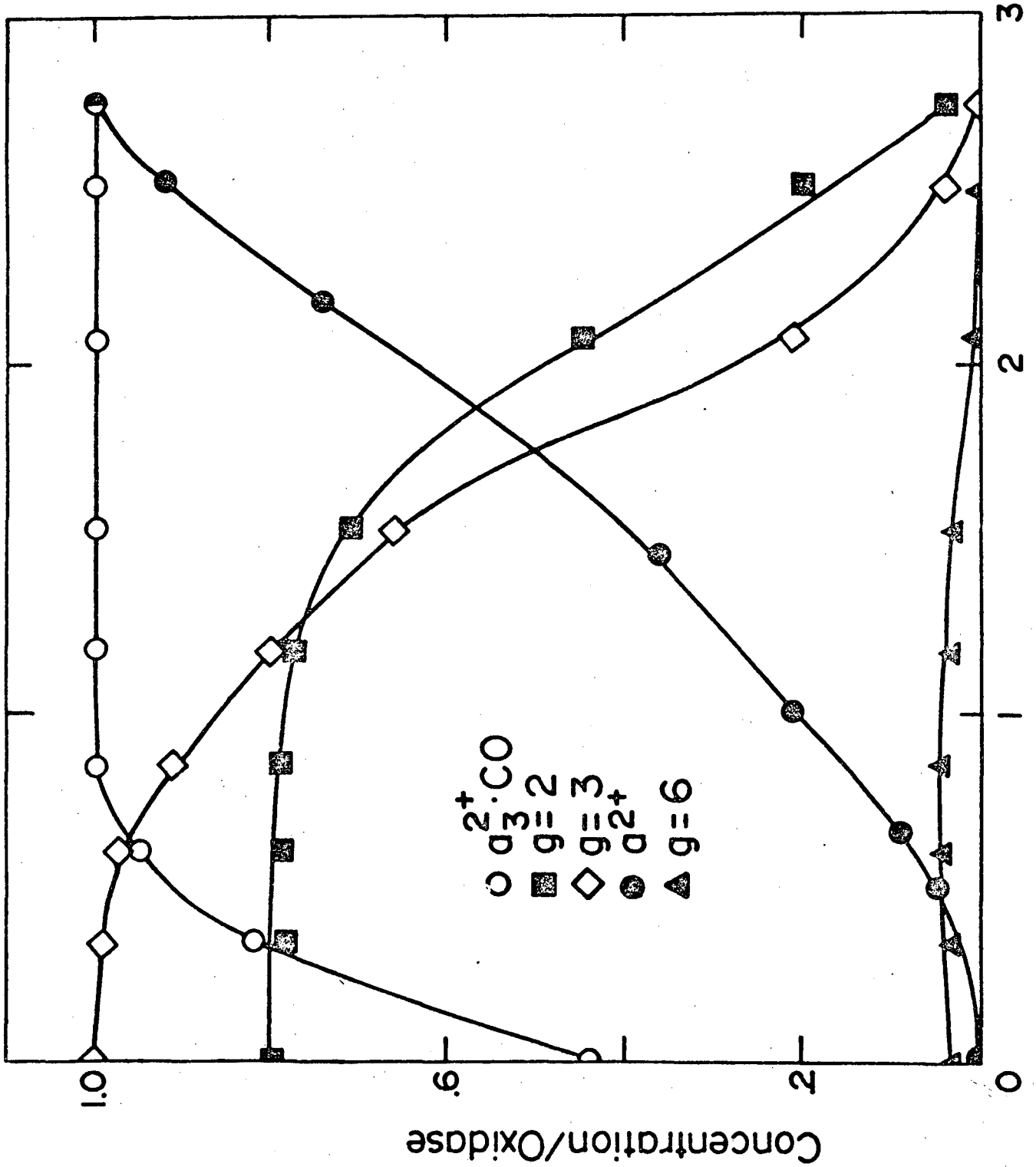

Fig. 11

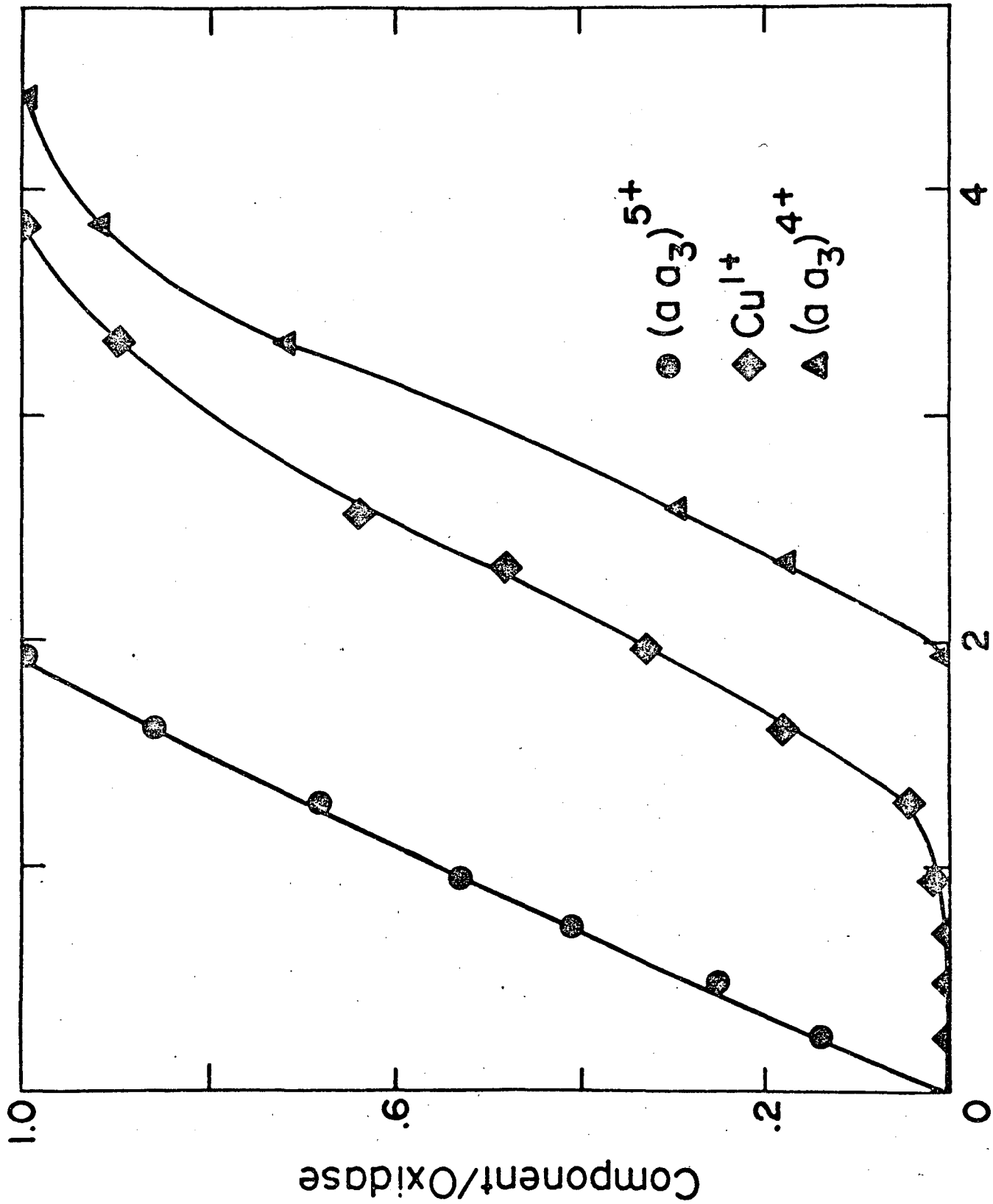

Fig. 12

This report was done with support from the Department of Energy. Any conclusions or opinions expressed in this report represent solely those of the author(s) and not necessarily those of The Regents of the University of California, the Lawrence Berkeley Laboratory or the Department of Energy.

TECHNICAL INFORMATION DEPARTMENT
LAWRENCE BERKELEY LABORATORY
UNIVERSITY OF CALIFORNIA
BERKELEY, CALIFORNIA 94720